Изучение осцилляций нейтрино в эксперименте NOvA

(Участие ОИЯИ)

Продление проекта на период 2018-2020 гг

Study of Neutrino Oscillations in NOvA experiment

(JINR Participation)

Project extension for the period 2018-2020

Шифр темы: 02-2-1099-2010/2018 Study of Neutrino Oscillations (Project NOvA)

Направление: Физика частиц и релятивистская ядерная физика

Авторы от ОИЯИ:

V.Allakhverdian[1], V.Amvrosov[1], N.Anfimov[1], A.Antoshkin[1], N.Balashov[3], A.Baranov[3], S.Bilenky[2], A.Bolshakova[1], A.Dolbilov[3], I.Kakorin[4], O.Klimov[1], L.Kolupaeva[1], C.Kullenberg[1], K.Kuzmin[2], E.Kuznetsov[3], V.Matveev[2], A.Morozova[1], V.Naumov[2], A.Olshevskiy[1], O.Petrova[1], O.Samoylov[1], A.Sheshukov[1], A.Sotnikov[1], D.Velikanova[1]

[1] Dzhelepov Laboratory of Nuclear Problems (DLNP)
[2] Bogolyubov Laboratory of Theoretical Physics (BLTP)
[3] Laboratory of Information Technologies (LIT)
[4] Veksler-Baldin Laboratory of High Energy Physics (VBLHEP)

Руководитель проекта: А.Г.Ольшевский

Зам.руководителя: О.Б.Самойлов

Дата представления проекта в НОО _____

Дата НТС Лаборатории   06/04/2017 (ЛЯП)

Номер документа _____

Дата представления физического обоснования

на семинаре Лаборатории: 03/03/2017(ЛЯП), 17/03/2017(ЛЯП), 05/04/2017(ЛЯП)

ЛИСТ СОГЛАСОВАНИЙ ПРОЕКТА

**Изучение осцилляций нейтрино в эксперименте NOvA
(Участие ОИЯИ)
Продление проекта на период 2018-2020 гг**

**Study of Neutrino Oscillations in NOvA experiment
(JINR Participation)
Project extension for the period 2018-2020**

Шифр темы: **02-2-1099-2010/2018**

Утвержден директором ОИЯИ   _____   _____
                                        подпись   дата

СОГЛАСОВАН

Вице-директором ОИЯИ   _____   _____

Гл.уч.секретарем ОИЯИ   _____   _____

Пом. директора по финансовым и
экономическим вопросам   _____   _____

Гл. инженером ОИЯИ   _____   _____

Директором Лаборатории   _____   _____

Гл. инженером Лаборатории   _____   _____

Руководителем проекта   _____   _____

О Д О Б Р Е Н

ПКК по направлению   _____   _____

1. Executive Summary

With the discovery of a non-zero θ_{13} mixing angle the neutrino physics has entered a new era of tackling the problems of neutrino mass hierarchy and lepton CP violation. Both questions can be addressed in accelerator-type long baseline experiments through the measurement of matter effects in atmospheric-regime neutrino oscillations.

NOvA is a new generation experiment studying oscillations of muon to electron flavor neutrinos. The NOvA apparatus consists of a Near Detector at the Fermilab site, where the muon neutrinos are produced by the NuMI facility, and a Far Detector placed 810 km away. Both detectors are of similar construction based on a large-volume liquid scintillator tracking calorimeter, and both are situated 14 mrad off-axis to the neutrino beam, optimizing the signal to background ratio.

The complete 14 kton Far Detector and 220 ton Near Detector have been taking data since 2014, and a number of important measurements have been performed on the basis of statistics collected so far: a ν_e appearance signal measurement has allowed for the restriction of the hierarchy-δ_{CP} parameter space, a ν_μ disappearance signal was measured confirming oscillation parameters Δm^2 and $\sin\theta$ with high precision, moreover, from the NOvA data the θ_{23} maximal mixing was excluded for the first time with ~3σ confidence level.

Continuing the data collection, and importantly, altering neutrino and anti-neutrino beams, NOvA can unambiguously resolve the neutrino mass hierarchy at >95% C.L. for over a third of possible values of δ. For other values of this CP violation parameter, NOvA will provide δ-dependent hierarchy determination plus improved measurements of θ_{13}, θ_{23}, $|\Delta m^2_{23}|$, and δ itself, which is also very important for global analysis of the neutrino oscillation data.

The JINR group in NOvA has contributed significantly to the NOvA results. The Remote Operation Center (ROC-Dubna) was developed at JINR, giving the possibility to fully participate in the data taking and quality monitoring. The JINR computer infrastructure on the basis of GRID and Cloud technologies was developed. It is efficiently used for the home-based running of jobs and is also a part of the NOvA distributed computing resources system for the use at peak loads (e.g., before conferences). The NOvA electronics test bench was set up at JINR and provided important measurements of electronics parameters used for simulation and calibration.

Members of the JINR group are deeply involved in the ongoing analyses and in the preparation of new ones. This comprises the ν_μ, ν_e, Supernova, Slow monopole, Cosmic Ray and Near Detector physics teams. They are also involved in the development of simulation and analyses software, and are serving as a Detector Simulation convener, Offline and DAQ Software Release Managers, DAQ, DDT and ROC experts, etc.

Further running of the NOvA experiment will provide very competitive data for the measurement of neutrino mass ordering, CP-violation effects, disentangling the octants of θ_{23}, among many others. There are also plans to extend NOvA data collection beyond 2020, which will further increase the physics potential of this experiment.

The JINR team is planning to continue and extend its involvement in the NOvA data taking and analyses. As a part of this work we are planning maintenance of ROC-Dubna and the hardware test bench facility, as well as a further increase of the NOvA computing power at JINR to cope with the large amount of data, and the continuation of the aforementioned analyses.

The work of NOvA at JINR attracts a lot of attention from students and young staff, which provides a good potential for growing and extending the JINR participation in this excellent physics.

The requested resources for the project from the JINR budget are: 80K$/year for Materials and Equipment and 50K$/year for visits to FNAL and participation in the conferences and other meetings.

2. Introduction

2.1. Physics Motivation

The <u>Nu</u>MI <u>O</u>ff-axis <u>v</u>$_e$ <u>A</u>ppearance (NOvA) is a two-detector, long-baseline, atmospheric-regime neutrino oscillation experiment designed to address a broad range of open questions in the neutrino sector through precision measurements of $\nu_\mu \rightarrow \nu_e$, $\nu_\mu \rightarrow \nu_\mu$, and $\bar{\nu}_\mu \rightarrow \bar{\nu}_e$, $\bar{\nu}_\mu \rightarrow \bar{\nu}_\mu$ oscillations.

Much of the NOvA's physics scope comes from the appearance channels, as the observed rates of ν_e and $\bar{\nu}_e$ interactions provide information on:

- the ordering of the neutrino masses (whether the ν_3 state is heavier or lighter than the other two)
- the amount of CP violation present in the neutrino sector
- the size of the PMNS mixing angle θ_{13}
- whether the ν_3 state has more ν_μ or ν_τ admixture (whether θ_{23} is > or < than 45 degrees)

Results by reactor $\bar{\nu}_e$ disappearance experiments demonstrating $\theta_{13} \approx 9°$ [1] ensure that NOvA will have substantial event rates in the appearance channels. Through ν_μ and disappearance measurements, the NOvA experiment will provide improved precision on the dominant atmospheric oscillation parameters θ_{23} and Δm_{atm}^2, which is of utmost importance for the global fits and understanding of the full neutrino oscillation scheme.

For all of the oscillation measurements, NOvA takes advantage of a two-detector configuration to mitigate uncertainties in neutrino flux, neutrino cross-sections, and event selection efficiencies.

Outside of the primary goals, NOvA will also look for evidence of new physics through comparisons of $\nu_\mu \rightarrow \nu_\mu$, provide constraints on sterile neutrino models by measuring the total flux of active neutrinos at its downstream detector, monitor for supernova neutrino activity, perform neutrino-nucleus cross section measurements with a narrow-band beam, and pursue a variety of non-neutrino topics including searches for magnetic monopoles and hidden sector particles.

2.2. Neutrino Source

The NOvA experiment uses Fermilab's NuMI beamline as its neutrino source. The NOvA detectors are situated 14 mrad off the NuMI beam axis, so, due to the kinematics of neutrino production in pion decays, they are exposed to a relatively narrow band of neutrino energies centered at 2 GeV. Figure 1 shows how the energy spectrum for ν_μ charged current (CC) events varies with detector position. The suppressed high-energy tail at NOvA's off-axis location reduces neutral current backgrounds in the visible energy range of 1 to 3 GeV where the appearance of ν_e CC events should occur.
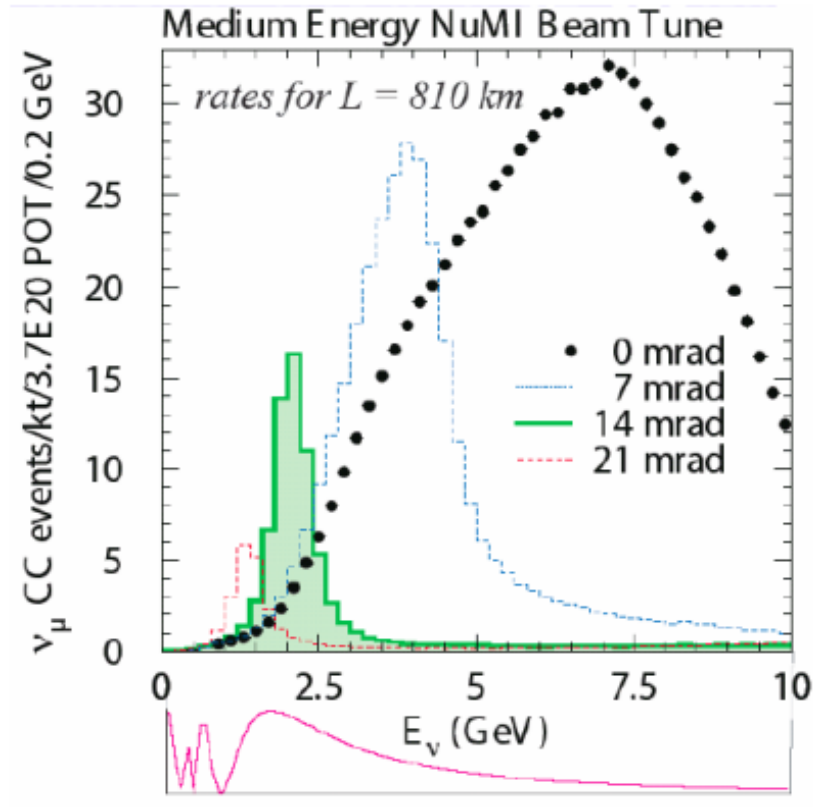
Figure 1. Beam spectra for off-axis "medium energy tune" NuMI beams with different off-axis angles. The dots show the on-axis beam and the shaded region shows the NOvA beam. The insert on the bottom shows the relative $\nu_\mu \rightarrow \nu_e$ oscillation probability as a function of energy.

At present the NuMI source underwent an upgrade to increase its average proton beam power from 350 kW to 700 kW. Much of the increased power comes from a reduction in the Main Injector cycle time, which drops from 2.2 seconds to 1.3 seconds. Conventional sensitivities of the NOvA experiment are estimated for 6 years of running at this stage of accelerator upgrade, where 6×10^{20} protons are delivered on the production target each year.

2.3. NOvA Detectors

The NOvA Far Detector (FD) is located off the Ash River Trail in northern Minnesota, 810 km from the NuMI target. The NOvA Near Detector (ND) is located on the Fermilab site about 1 km from the NuMI target.

Neutrino oscillations are studied by comparing events in the near detector, where the neutrinos have not yet had time to oscillate, with those in the far detector. Using this comparison greatly reduces the systematic error, since uncertainties in the flux, cross sections, and hadronic interactions largely cancel in the comparison.

The NOvA detectors can be considered as totally active, tracking, liquid scintillator calorimeters. A NOvA cell is a PVC tube of $155\times6\times3.9$ cm^3 filled with liquid scintillator. Light from the scintillator is captured by the fibers and is transmitted to the APD. Fibers from 32 cells (module) are grouped on one APD board (See Fig. 2). Each plane is made up of twelve modules and the planes alternate in having their long dimension horizontal and vertical. The FD consist of 896 planes, corresponding to a total mass of ~14 kt.

Figure 2. General concept of the NOvA detectors design

The NOvA ND is identical to the far detector except that it is smaller. The length of the tubes is scaled down to the ND transverse size of 4.1 m, but the longitudinal and transverse segmentations are the same as for FD. Additional details of the NOvA detectors design can be found in the Technical Design Report [2].

3. NOvA Results and Plans

3.1. Data Taking Summary

The NOvA experiment started data taking on 6 February 2014 with 4 diblocks in the Far Detector, out of 14 planned (see Fig. 3). The detector construction was finally finished on 29 July 2014 and only since then the full detector operation has started. Therefore the exposure presented below is sometimes defined in terms of POT (Protons On Target) flux equivalent to the full detector configuration.
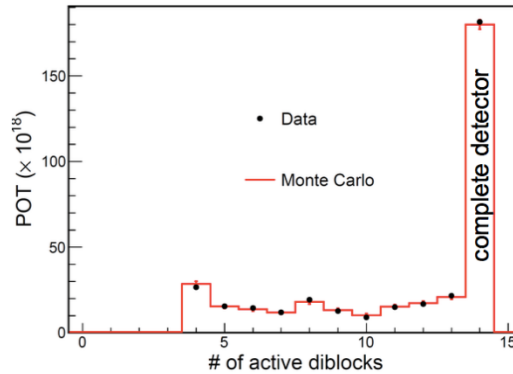
Figure 3. Data taking during commissioning of the NOvA Far Detector

A recent NOvA analysis [3,4] was performed with 6.68×10^{20} protons delivered by NuMI to the carbon target until 02 May 2016. After normalizing to the full detector size it is equivalent to 6.05×10^{20} POT. This is equal to ~1 nominal NOvA project year where the beam reaches 700 kW. Planned beam power (700 kW) was steadily reached in 2016 due to substantial efforts by the Fermilab Accelerator Division. The total number of POT delivered to the target and accelerator beam power for different periods of exposure are presented in the Figure 4.
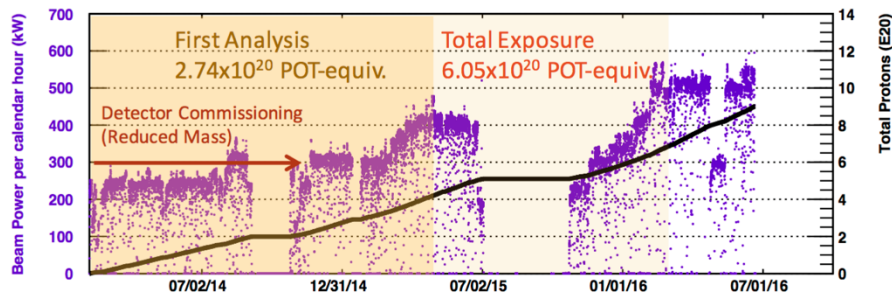
Figure 4. Integrated POT flux and NuMI beam power.

In this analysis period the Near Detector accumulated 3.72×10^{20} POT of good data.

3.2. ν_μ Disappearance

Significant improvement in the recent analysis was accomplished with the upgrade of the NOvA version of GENIE from 2.8.6 to 2.10.4. The main impetus for the upgrade was to obtain a basic model of neutrino interactions with di-nucleon pairs in the nucleus (2p2h or "MEC" events). On the recommendation of the hadronic energy task force the so-called "MEC" process has been turned on in our simulation and further weighting was applied. This is an essential part of the hadron energy prediction. In the following Figures 5 and 6 one can see the importance of MEC interactions for NOvA.

8
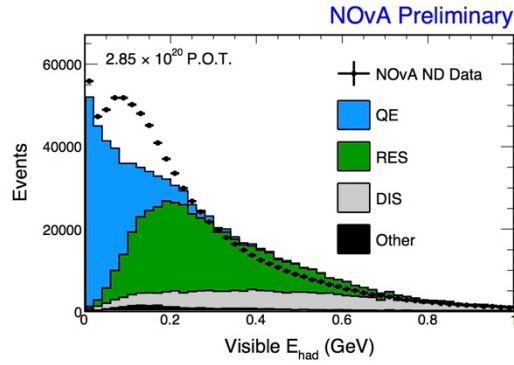
Figure 5. Visible hadronic energy in selected charged-current muon neutrino interactions in the Near Detector. Colored histograms correspond to the predicted true interaction types from GENIE 2.10.2 ("QE" is QuasiElastic scattering; "RES" is Resonant production; "DIS" is Deep Inelastic Scattering). Data points are ND data with statistical uncertainties (2.85×10^{20} POT).
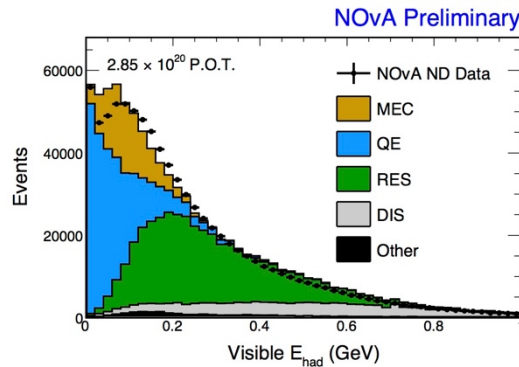
Figure 6. Measured visible hadronic energy (see also Fig. 5 for explanations) compared to the model with additional GENIE MEC component reweighted as mentioned in the text.

The muon disappearance analysis uses a special particle identification tool called the ReMId kNN-based identifier. The calculation of the probability of a track being a muon is based upon the topological qualities of the reconstructed track. As input values it uses dE/dx Log-Likelihood, Scattering Log-Likelihood, Track Length, and Non-hadronic Plane Fraction. Log-Likelihoods are calculated under different particle assumptions. The final PID variable is formed as output of a kNN classifier. Distributions of the ReMId PID variable for the Near detector using recent analysis files are shown in the Figure 7.
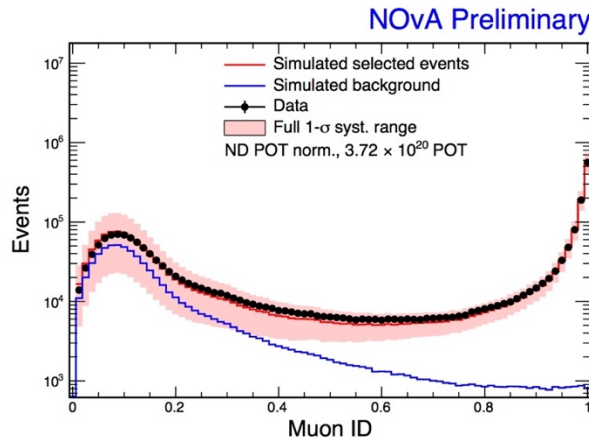
Figure 7. ND FHC distributions, data and MC with full systematics band, for ReMId, POT normalized.

One of the most complicated issues for the muon disappearance analysis is the rejection of the cosmic muon background. For a successful analysis we need a 99.9999% rejection of cosmics. For that purpose the Boosted Decision Tree (BDT) algorithm is used. The philosophy is as follows: reject background events with simple cuts and use the remaining sample to train BDT, that can take into account all the information and correlations amongst the many various discriminating variables. The BDT output is shown in the Figure 8. The difference between signal and background is very clear.
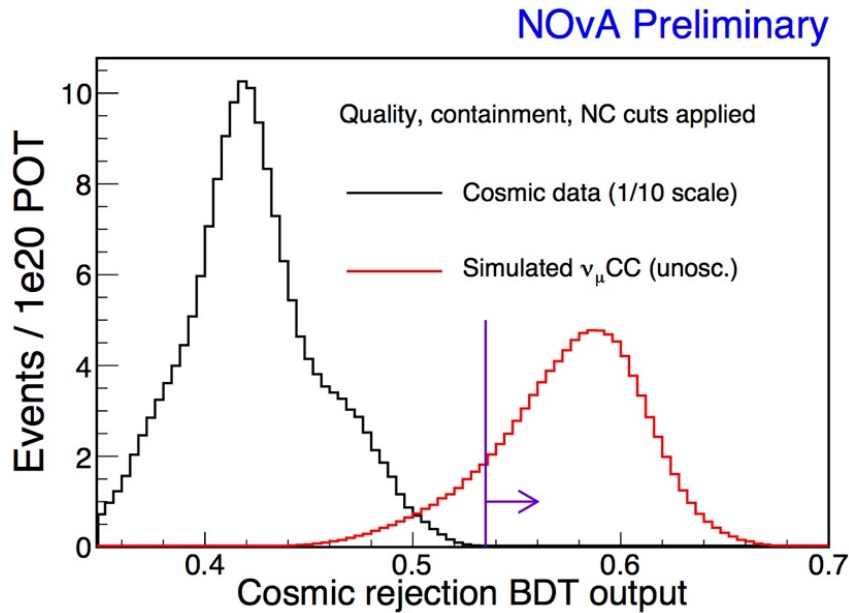
Figure 8. ND FHC distributions, data and MC with shape-only systematics band, for ReMId, area normalized.

The rejection power of all numu analysis cuts can be seen in the Figure 9.
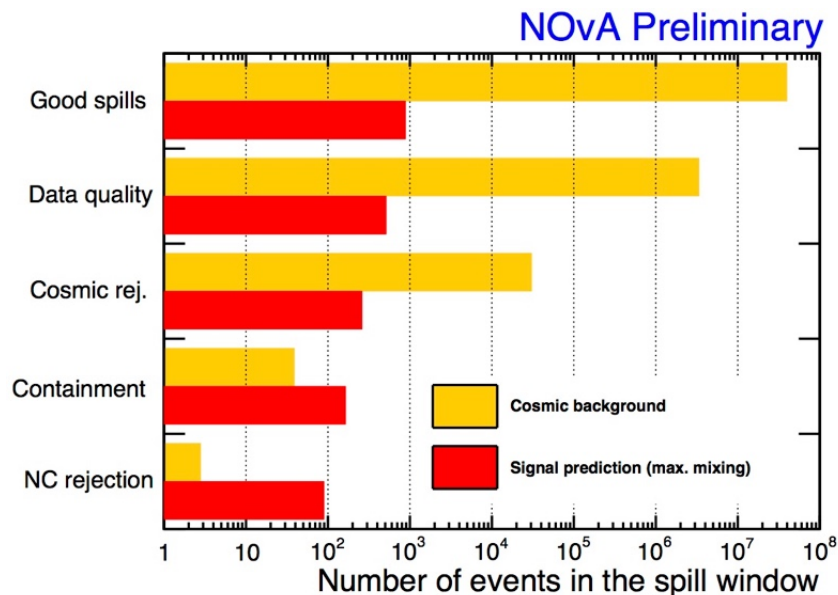
Figure 9. Number of cosmic background events (yellow), from out of time sideband, and number of signal events (red), from MC, surviving after each analysis cut is applied.

Systematic uncertainties for this analysis are presented in Table 1.

Source of uncertainty	Uncertainty in $\sin^2\theta_{23}(\times 10^{-3})$	Uncertainty in Δm^2_{32} $(\times 10^{-6}$ eV$^2)$
Absolute muon energy scale [$\pm 2\%$]	+9 / -8	+3 / -10
Relative muon energy scale [$\pm 2\%$]	+9 / -9	+23 / -14
Absolute hadronic energy scale [$\pm 5\%$]	+5 / -5	+7 / -3
Relative hadronic energy scale [$\pm 5\%$]	+10 / -11	+29 / -19
Normalization [$\pm 5\%$]	+5 / -5	+4 / -8
Cross sections and final state interactions	+3 / -3	+12 / -15
Neutrino flux	+1 / -2	+4 / -7
Beam background normalization [$\pm 100\%$]	+3 / -6	+10 / -16
Scintillation model	+4 / -3	+2 / -5
δ_{CP} [$0 - 2\pi$]	+0.2 / -0.3	+10 / -9
Total systematic uncertainty	+17 / -19	+50 / -47
Statistical uncertainty	+21 / -23	+93 / -99

Table 1. Sources of uncertainty and their estimated average impact on the $sin^2\,\theta_{23}$ and Δm^2_{32} measurements. For this table, the impact is quantified using the increase in the one-dimensional 68% C.L. interval, relative to the size of the interval when only statistical uncertainty is included in the fit. Simulated data were used and oscillated with $\Delta m^2_{32} = 2.67 \times 10^{-3}$ eV^2 and $sin^2\,\theta_{23} = 0.626$.

In this analysis 78 ν_μ CC events were detected with an expected background of 3.4 NC, 0.23 ν_e CC, 0.27 ν_τ CC and 2.7 cosmic events. Their FD spectra are shown in the Figure 10.
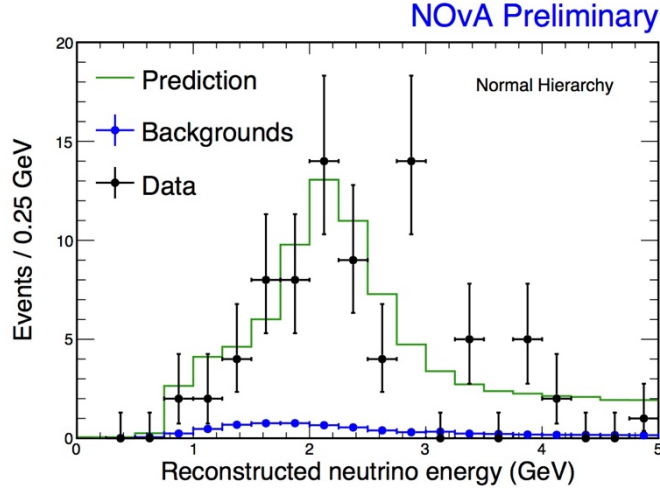
Figure 10. ν_μ final spectrum showing data and best fit prediction.

The best fit to the data gives:
1. $\Delta m^2_{32} = (+2.67 \pm 0.11) \times 10^{-3}$ eV^2 and $sin^2\,\theta_{23}$ at two statistically degenerate values $0.404^{+0.030}_{-0.022}$ or $0.624^{+0.022}_{-0.030}$ both for Normal Hierarchy.
2. For Inverted Hierarchy $\Delta m^2_{32} = (-2.72 \pm 0.11) \times 10^{-3}$ eV^2 and $sin^2\,\theta_{23} = 0.398^{+0.030}_{-0.022}$ or $0.618^{+0.022}_{-0.030}$.

The best fit has χ^2/d.o.f = 41.6/17, which arises mainly from bins in the tail of energy spectrum (with a little information about 3 flavor oscillations). The fit in the restricted region with data below 2.5 GeV gives the same parameter values and reduces the χ/d.o.f to 3.2/7.

The best fit for Δm_{32}^2 and θ_{23} is shown in the Figure 11. An additional Figure 12 shows a comparison with other experiments.
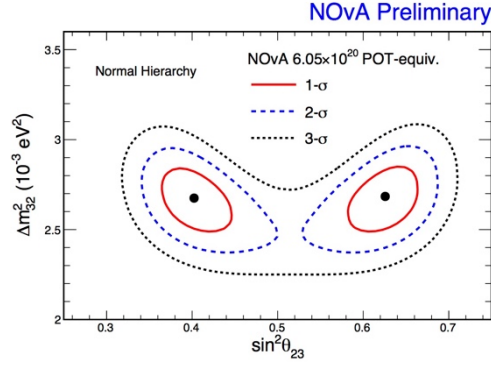
Figure 11. ν_μ contours for normal hierarchy showing 1, 2, and 3σ with systematics.
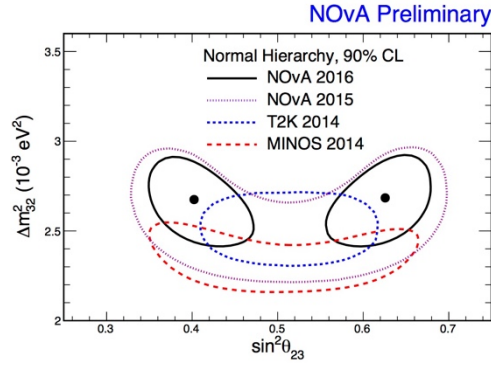
Figure 12. 90% CL contours for NOvA ν_μ overlaid with recent T2K and MINOS results.

As a result of the present NOvA ν_μ analyses, maximal mixing for θ_{23} was disfavored at a 2.6σ level for the first time.

3.3. ν_e Appearance and Combination with ν_μ

NOvA Far Detector (FD) analyses use the Near Detector (ND) for the prediction of event spectra in the FD after oscillations. An extrapolation procedure is used for this purpose. The procedure is presented schematically in the Figure 13.
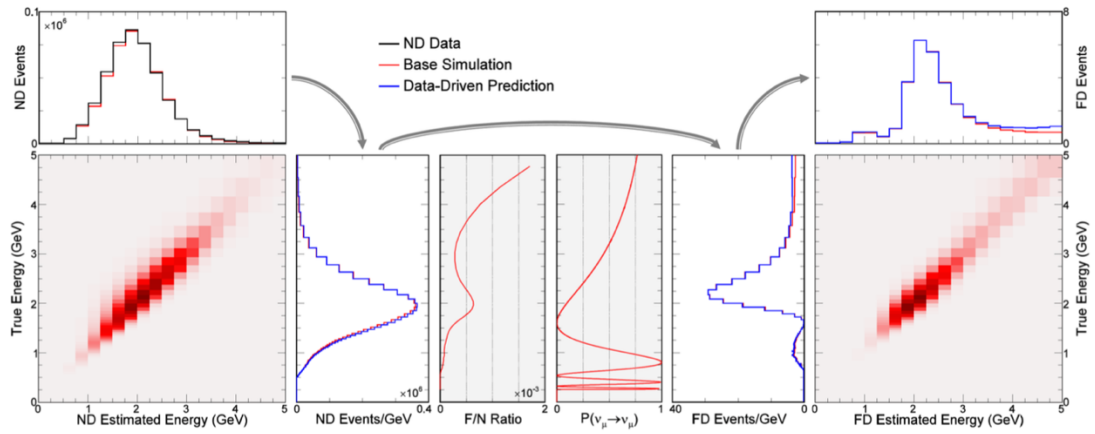
Figure 13. Schematic view of ND/FD extrapolation procedure.

The main steps of the extrapolation procedure (from top left) are:
1. Estimate the true energy distribution of selected ND events.
2. Multiply by expected FD/ND event ratio and oscillation probability as a function of true energy.
3. Convert the FD true energy distribution into a predicted FD reconstructed energy distribution.

Systematic uncertainties are assessed by varying all MC-based steps.

The analysis channel is ν_e Charge Current (CC). Thus the main goal of the ν_e analysis is the identification of events with electromagnetic showers and the suppression of the background, in particular, cosmic events. Events selected in the Far Detector pass through a series of cuts. Among them are Fiducial and Containment cuts, Shower length, Calorimetric energy, and Reconstructed pT/p among others. Selection criteria for the presented analysis were optimized by maximizing FOM (Figure Of Merit = S/$\sqrt{S + B}$, where "S" stands for signal and "B" is background.

The cuts used in the analysis are extremely efficient in rejecting background: with a toll of 50% on our signal events we reject 98.3% of the beam background and practically all cosmic background. In the end our analysis sample has only 0.5 cosmic events, rather than 1.6×10^6, and 8.2 total beam background events, as opposed to the 418 initial events. The expected number of pure signal after all cuts is ~25 events.

This rejection power was impossible without our new event classification algorithm, the Convolutional Visual Network (CVN), which is based on ideas from computer vision and deep learning. This is NOvA's adaptation of traditional Convolutional Neural Networks (CNN). This CNN takes a calibrated hit map as inputs and constructs a pair of "images" describing the event, one for the X view, and another for the Y view, which are passed through the network. The Multi Layer Perceptron at the end of the network uses the feature map extracted by the CNN to create a classifier output for each of (ν_μ CC, ν_e CC, ν_τ CC) times (QE, RES, DIS, Other). The work of the CVN algorithm is schematically depicted in the Figure 14.
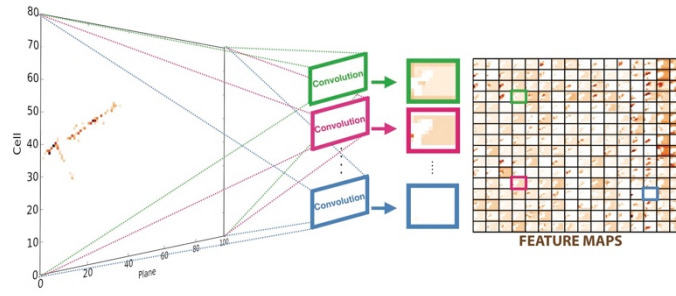
Figure 14. The scheme of the CVN algorithm operation.

The output of the CVN is a value of PID (Particle IDentification number) varying from 0 to 1, which describes the nue CC – likeness of the event: 0 is a pure background, 1 is a pure signal event. The CVN PID values for selected events are presented in the Figure 15.
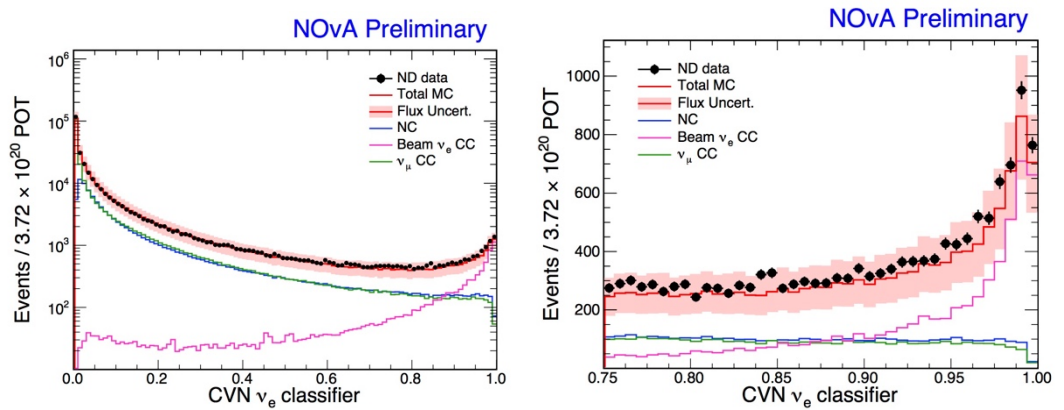
Figure 15. Selected ND events over CVN PID values.

Events with CVN PID higher than 0.75 are selected to participate in further analysis. Their reconstructed neutrino energy spectrum is presented in the Figure 16.
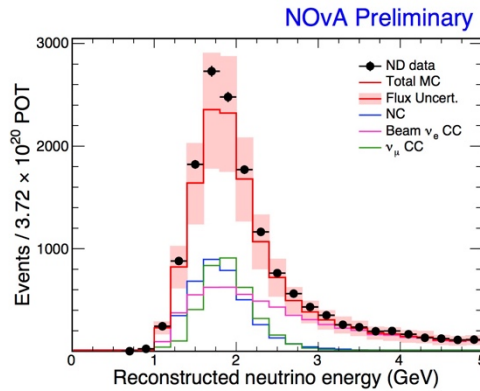
Figure 16. Reconstructed neutrino energy spectrum of ND events with PID>0.75.

Events are further classified according to their PID and initial neutrino energy: PID is divided into 3 bins (0.75, 0.87), (0.87, 0.95) and (0.95, 1), and energy bins have a width of 0.5 GeV. The corresponding spectra of events are presented in the Figure 17.
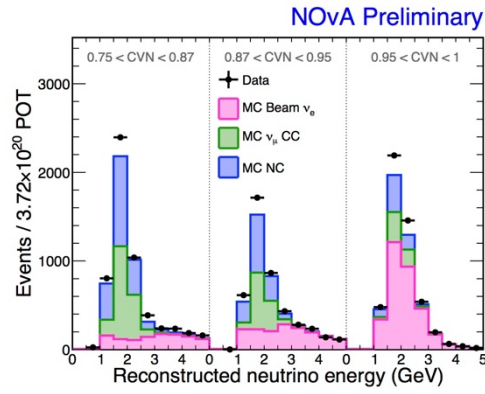
Figure 17. Reconstructed neutrino energy spectra of ND events for different PID bins.

The ND spectra are translated to the FD bin by bin using the extrapolation procedure described above. However, in the ND spectra one may notice a ~10% discrepancy between data and MC. Therefore, an additional tuning was applied. Beam composition in the ND is ν_μ CC, ν_e CC and NC. All of these are also sources of background in the FD. It is extremely important to know the correct beam composition and in order to correct our MC with appropriate weights two decomposition techniques were implemented.

The first one is the BEN decomposition, that works with ν_e CC component. The source of neutrinos are decayed mesons that were produced in the target. The fitting of the ND data with the MC predicted spectra (see Figure 18) of all neutrino ancestors provides the weights for each of ancestor mesons. This reweighting causes an increase in ν_e CC of +1%.
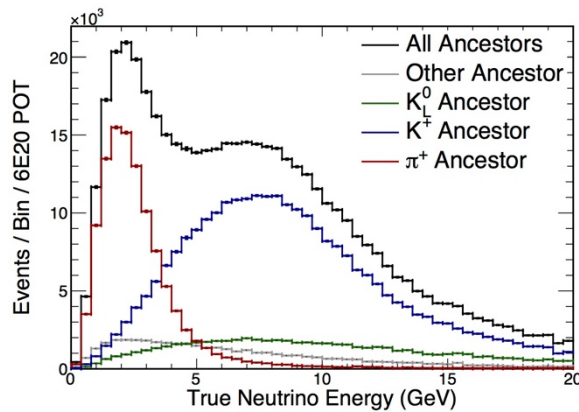
Figure 18. Contribution of different ancestors to the neutrino spectrum.

Weights for ν_μ CC and NC are obtained by Michel decomposition. The ν_e CC component remains fixed after the first decomposition. The spectra of Michel electrons measured in the ND are fitted with MC. A ν_μ CC interaction should have +1 Michel electron in comparison with nue CC and NC. This technique gives +17.4% in ν_μ CC and +10.4% in NC. The final spectra with reweighted MC are presented in the Figure 19.
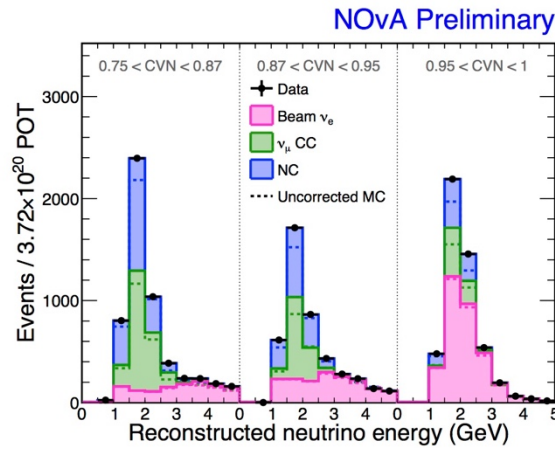
Figure 19. Reconstructed neutrino energy spectra of ND events for different PID bins after tuning.

The systematic uncertainties in FD predictions were estimated by changing relevant systematic sources one by one within ±1σ. The main sources that were considered are:

1. calibration procedures, both variation in the calibrated detector response across the X and Y views and the overall energy scale, taken as a relative (uncorrelated) and absolute (correlated) effect between the two detectors.
2. numerous parameters of the GENIE simulation of neutrino interactions, those with the largest impact on the final Far Detector signal or background predictions (M_A the Llewellyn-Smith, M_A in the Rein-Sehgal Coherent model, Pauli blocking momentum cutoff etc)
3. uncertainties in the neutrino flux arising from hadron production uncertainties.
4. uncertainty from the simulation of scintillator quenching (Birks' parameter).
5. uncertainty on the relative far/near normalization from uncertainties in POT accounting and the detector masses, Near Detector-specific intensity effects, and variations in the prediction depending on the ND fiducial volume.

Summary plots for signal and background uncertainties are presented in Figure 20. We end up with a 5% total systematic uncertainty on signal and 10% on background.
For both cases statistical error still dominates.
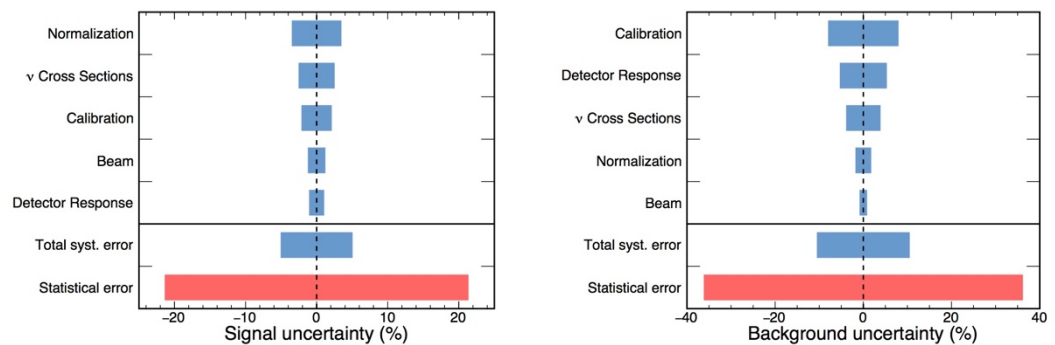
Figure 20. Signal (left) and background (right) uncertainties.

Our predictions for the number of events are presented in Figure 21.

Figure 21. Total number of events expected in the Far Detector as a function of δ_{CP} for NH (blue) and IH (red), with fixed $0.4 < sin^2\,\theta_{23} < 0.6$.

The Figure 22 demonstrates the principle by which NOvA determines the mass hierarchy and measures the δ_{CP}. NOvA essentially measures two oscillation probablities, one in neutrino mode (a point on the x-axis) and one in anti-neutrino mode (a point on the y-axis). The ellipses show the δ_{CP} values and choice of hierarchy that could yield from the oscillation probability measurements given a $sin^2\,2\theta_{23}$ value of 0.09. One can imagine that NOvA makes a measurement of oscillation probability in each neutrino mode that yields the starred point.

Figure 22. Oscillation probabilities in NOvA case. The blue curves are for the normal hierarchy and the red curves are for the inverted hierarchy. On each ellipse, the choice of the δ_{CP} varies as one moves around the ellipse as indicated by the symbols. This assumes maximal maxing in the θ_{23} octant. Stars are corresponded to smaller/larger ν_e rates (and opposite in $\bar{\nu}_e$ case).

We expect for signal: in case of IH and δ_{CP} = π/2 - 19.4 events
                            in case of NH and δ_{CP}=3π/2 - 36.4 events
For background we expect a total of 8.2 events (3.1 for beam ν_e CC, 3.7 for NC, 0.7 for ν_μ CC, 0.1 for ν_τ CC and 0.5 for cosmic events) and small variations with oscillation parameters.

In total, 33 ν_e CC events were observed. Their reconstructed neutrino energy distribution is presented in the Figure 23 for different bins of PID. Our observation is certainly towards the higher end of expectations.

Figure 23. Nue SA Energy vs PID distribution of FD selected events in data and MC prediction. This MC prediction uses the best fit parameters for Normal Hierarchy.

Also shown in Figure 23 is the best fit of our data, from which we can extract limits on the fitted parameters (see Figure 24). One can see that the ν_e only data are not so sensitive to the parameters yet.
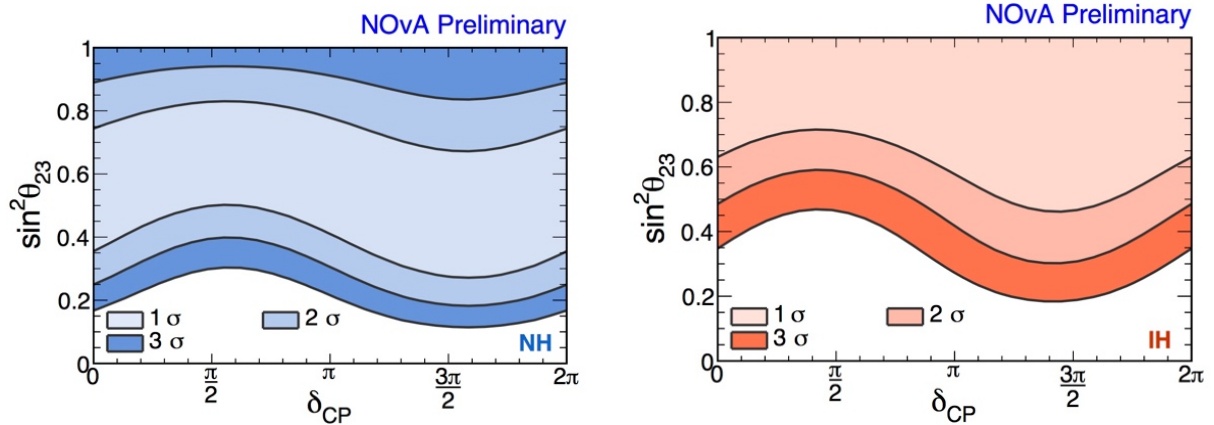
Figure 24. 1, 2 and 3σ allowed regions in $sin^2\theta_{23}$ space for normal (left) and inverted (right) hierarchy, as a function of δ_{CP}. No Feldman-Cousins corrections are applied. Signal and background systematics are taken into account.

In order to improve sensitivity, the joint fit for ν_e and ν_μ NOvA analyses was performed for the first time. The results are presented in the Figure 25.
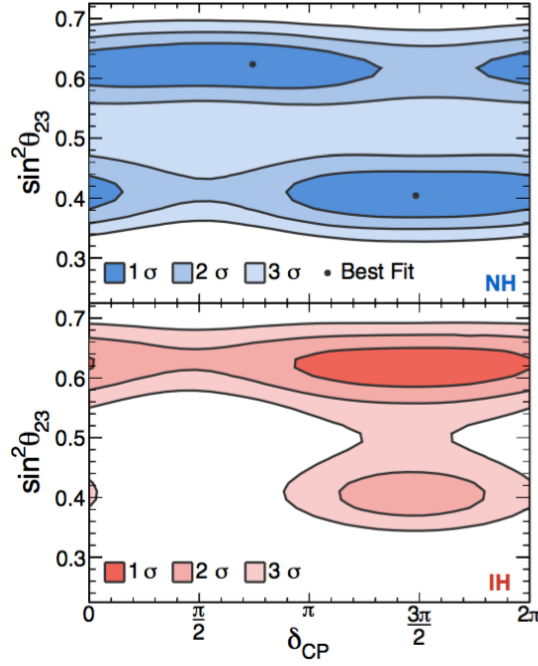
Figure 25. 1, 2 and 3σ allowed regions using numu constraint in $sin^2 \theta_{23}$ vs δ_{CP} for normal (top) and inverted (bottom) hierarchy. No Feldman-Cousins corrections are applied.

The present best fit equally prefers two points for NH:
1. $\delta_{CP} = 1.48\pi$, $sin^2 \theta_{23}= 0.404$ (Lower Octant (LO))
2. $\delta_{CP} = 0.74\pi$, $sin^2 \theta_{23}= 0.623$ (Upper Octant (UO))

Currently the data slightly prefer the Normal Hierarchy. The difference in the best fit for NH and IH is 0.46σ. But we have already excluded a region in IH, Lower Octant, around $\delta_{CP} =\pi/2$ at 3σ and LO at greater than 93% C.L. for all values of δ_{CP}.

The significance at which the values of δ_{CP} are disfavored for each of the four possible combinations of MH and θ_{23} octant is presented in the Figure 26.
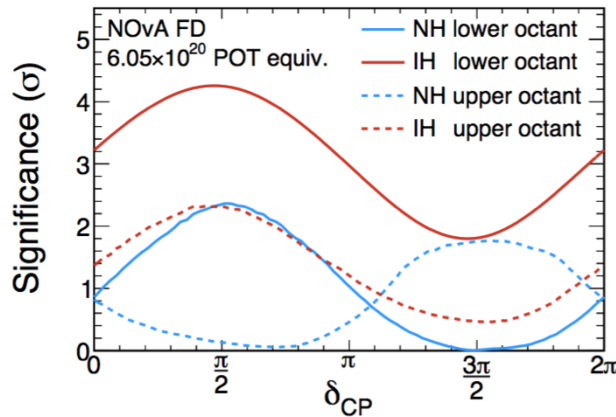
Figure 26. Significance as a function of δ_{CP} for NH (blue) and IH (red), with fixed $sin^2 \theta_{23}=0.4$ (solid) and $sin^2 \theta_{23}=0.6$ (dotted). Feldman-Cousins corrections are applied. Signal and background systematics are taken into account. Δm_{12}^2 and $sin^2 \theta_{13}$ are held within global uncertainties.

19

Confusion in octants of θ_{23} tangle the measurement of mass hierarchy and δ_{CP}. In other words, in terms of oscillation probability we have results for both octants. In order to resolve such difficulty we need an antineutrino run. This is explained in the Figure 27.
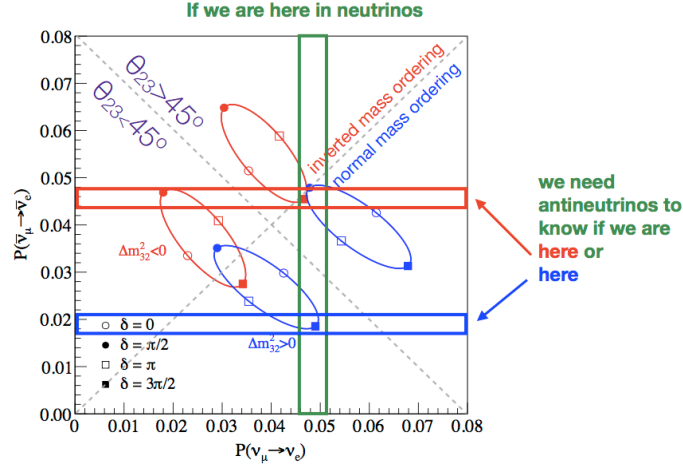
Figure 27. NOvA nue Bi-probabilities splited by θ_{23} octant non-maximal values.

NOvA gathered neutrino data until February 2017 (up to $9{\times}10^{20}$ POT) and then switched to antineutrinos. We will run in antineutrino mode until the next spring (up to $9{\times}10^{20}$ POT). This summer the analysis will be performed with only neutrino data, but in the summer 2018 the results for both samples will be presented.

3.4. Prospects for NOvA Sensitivities

At the beginning of NOvA's operation the potential of the experiment was estimated as follows:
    1. For Mass Hierarchy (MH) determination:
In the best case ($\delta_{CP} = \pi/2$ for IH and $3\pi/2$ for NH) NOvA will measure MH with sensitivity 3σ.
Unlucky regions: $\delta_{CP} = \pi/2$ for NH and $3\pi/2$ for IH.
    2. For CPV measurement:
In the best case (the same points) NOvA will measure CPV with sensitivity $\sim 1.5\sigma$.
Unlucky regions: $\delta_{CP} = 0$ (or 2π) and π.
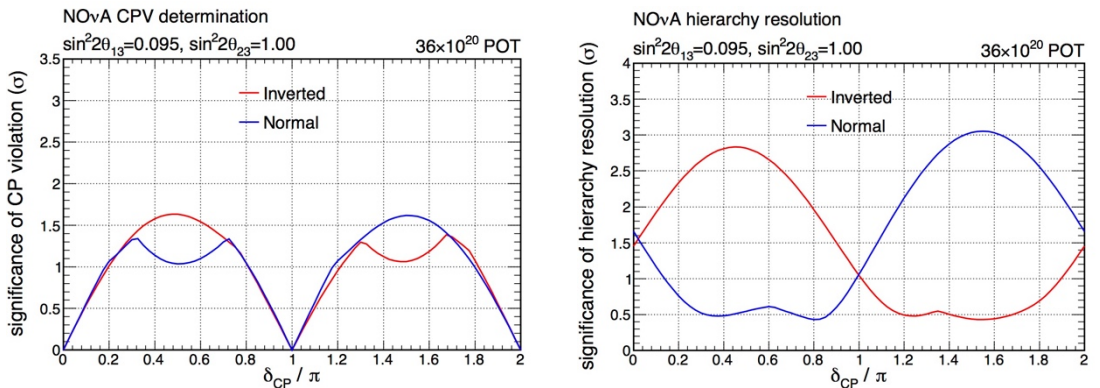
Figure 28. CPV (top) and MH (bottom) sensitivities of NOvA experiment estimated for 6 nominal project years.

All estimations above were performed with the assumption that NOvA will operate until 2020 and collect $36{\times}10^{20}$ POT equally distributed between neutrino and antineutrino runs. Today this number is considered as the minimum flux, which the NOvA experiment can expect.

Comparison of this minimum NOvA MH sensitivity with other world projects, aiming to measure MH, is presented in the Figure 29.
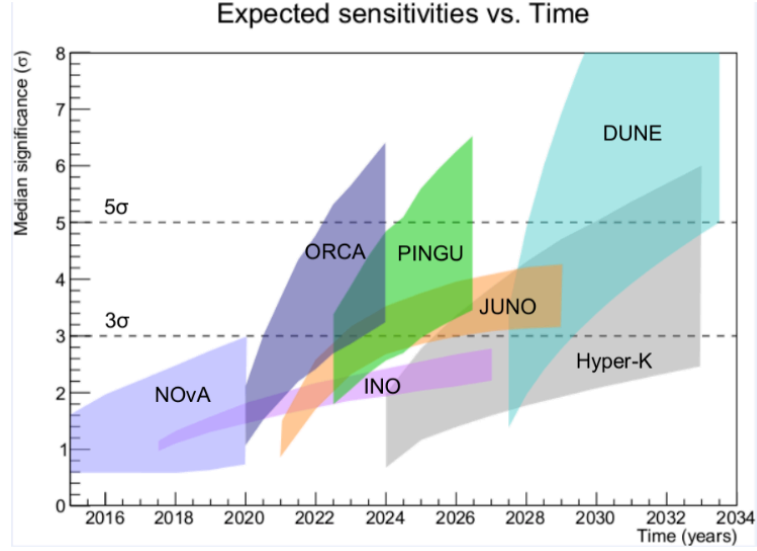
Figure 29. Expected time scale sensitivities for going and future neutrino experiments.

However, in addition to providing this minimum, the FNAL Accelerator Division is now developing a plan to steadily increase the proton beam power by upgrading and tuning existing accelerators up to ~1MW in the years 2020-2024. This opens new physics possibilities for NOvA operation.

Below we have made estimations for the current analysis techniques and extrapolate it for the next 8 years (collecting in total 54×10^{20} POT). Predictions are slightly different for the lower and upper θ_{23} octant cases, but even for the "worst" case of low octant there is a significant increase of experimental sensitivities and a possibility of providing competitive and timely measurements.
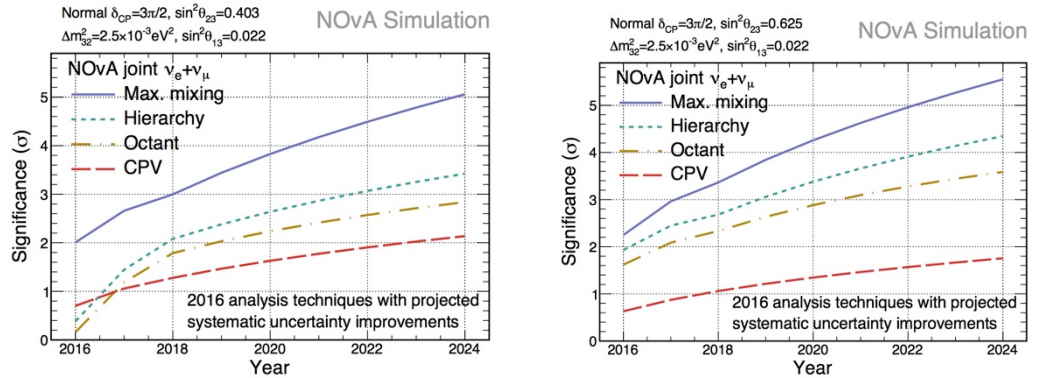
Figure 30. Projected sensitivities to rejection of: maximal mixing (violet), wrong hierarchy (green), wrong octant (yellow), and CP conservation (red), assuming true oscillation parameters NH, $3\pi/2$ and $sin^2\theta_{23}$=0.403 (left), $sin^2\theta_{23}$=0.625 (right). Joint fit combines the electron neutrino appearance and muon neutrino disappearance channels, and global reactor constraint $sin^2 2\theta_{13}$=0.085±0.005. Assuming 6×10^{20} POT delivered each year. The accumulated exposure is divided between FHC and RHC mode as: i) 6×10^{20} FHC by 2016, ii) 9×10^{20} FHC + 3×10^{20} RHC by 2017, iii) 9×10^{20} FHC + 9×10^{20} RHC by 2018, iv) 50% FHC + 50% RHC after that.

In summary, for the next several years NOvA can obtain:
1. For θ_{23}:
   2018 year – >3σ exclusion of maximal θ_{23}
   2019 year -- > 2σ octant determination
   2024 year --- >5σ exclusion of maximal θ_{23}
                  > 3σ octant determination
2. For Mass Hierarchy:
   2018r -- >2σ MH determination
   2020 year -- >3σ MH determination
3. For CP phase:
   2023 year -- >2σ CPV determination

We would like to emphasize that all estimations for NOvA mentioned above were done with the current analysis techniques of the experiment. All further improvements to the analysis methods will increase sensitivities for the θ_{23}, MH and CPV measurements. Therefore, these estimations are only the lower limit of our potential.

4. NOvA at JINR

4.1. Data Taking and Quality Checking

The NOvA experiment at both the ND and FD sites have storages and file transfer systems to accumulate detector data. While this is safely done at the FD and ND locally, it is more efficient to monitor the operation of both systems from one location simultaneously, which can be accomplished from a Remote Operation Center (ROC). This policy was anticipated from the very beginning for all neutrino experiments at FNAL, and now all of the NuMI experiments are developing ROCs. The Main Remote Operation Center, ROC-West, is located in the Wilson Hall at FNAL.

Currently twelve ROCs are operating for the NOvA experiment at different locations. The first non-US Remote Operation Center, ROC-Dubna, has been developed at JINR and started operation in October 2015. It has all of the necessary features and allows for full monitoring and control of FD and ND operation, as well as communication with FNAL services and other ROCs. Figures 31-32 show the general view of the ROC-West and ROC-Dubna.

Figure 31. ROC-West view.

Figure 32. ROC-Dubna view.

The NOvA experiment is operating 24/7 over its lifetime. (According to the project plan NOvA will run at least until the end of 2020). All of the ROCs together ensure continuous monitoring and control of detector systems on both sites, as well as monitoring of the beam status.

This work is managed by 3 Run coordinators changing every 2 weeks, which communicate with Shifters, ROC Contacts, System Experts and FNAL and Ash river On-site Crews. Such an organization allows for the smooth operation and monitoring of all system components: beam, detector, electronics, DAQ, data transfer, safety matters, etc.

The ROC-Dubna configuration is schematically presented in Figure 33.
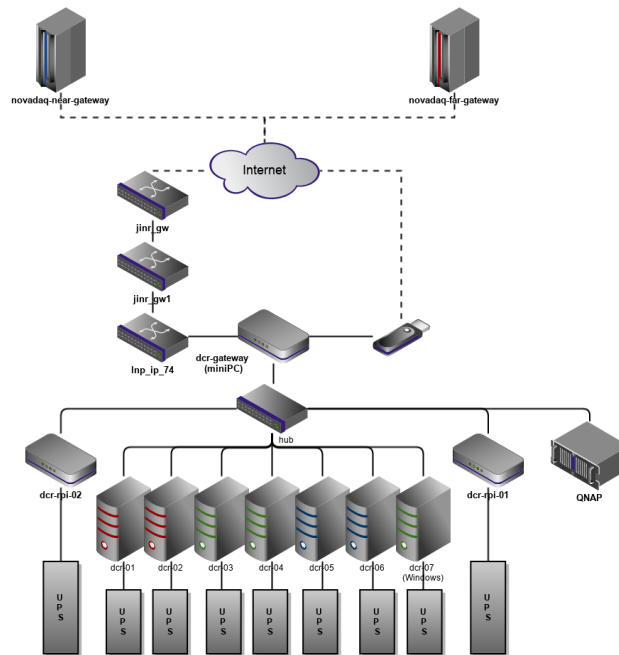
Figure 33. ROC-Dubna internet connection system.

NOvA data storage and transfer software is based on Linux-nodes, which collect information from NOvA DAQ system (not shown on the Figure) and provide it to the outside world through FD and ND gateway servers.

Each of the ROCs connect to the control and operation nodes on both FD/ND sites via VNC-tunneling under secure protocols. The basic idea is that a VNC server transfers a VNC session to many VNC viewers at ROCs with control. In total there are 5 active Scientific Linux based VNC-sessions, which are connected directly to Near/Far Detectors nodes and provide information further through gateways. The system also includes 1 Linux node for Web-monitoring of the operated systems (Beam, ND/FD Cameras, Data transfer control, Ganglia, Nearline) and 1 Windows node for communication (NOvA electronic logbook, Expert contacts and Bulletin Board, Polycom Vidyo, Slack-chat, Skype). We also have our own gateway to ensure a stable internet connection. The main idea is to monitor the existing connection constantly, and, in case of failure of the main ethernet connection, switch to a mobile 4G modem.

Figure 34. Internet path from ROC-Dubna to Fermilab.

The developed infrastructure of the ROC-Dubna allows for non-interruptible continuous work, which is necessary during shift periods. This infrastructure comprises: stable and backed up internet connection, communication tools including the international land-line, kitchen, etc. A computing monitoring system, based on Nagios, controls the ROC-Dubna local Linux-nodes, internet connection, server conditions, and notifies JINR experts in case of trouble.

ROC-Dubna is often showcased during excursions to the Laboratory by students, mass-media, and other visitors. Its presence at JINR has significantly increased the interest in the NOvA experiment by young people.

4.2. Hardware Tests

It was realized from the very beginning that the comprehensive understanding of the NOvA detector's operation will, in particular, require additional precise measurements of electronics parameters even after commissioning. For this reason an electronics test bench was developed at JINR using the components of actual NOvA electronics.

The NOvA test bench at JINR consists of a few parts (see Figure 35).
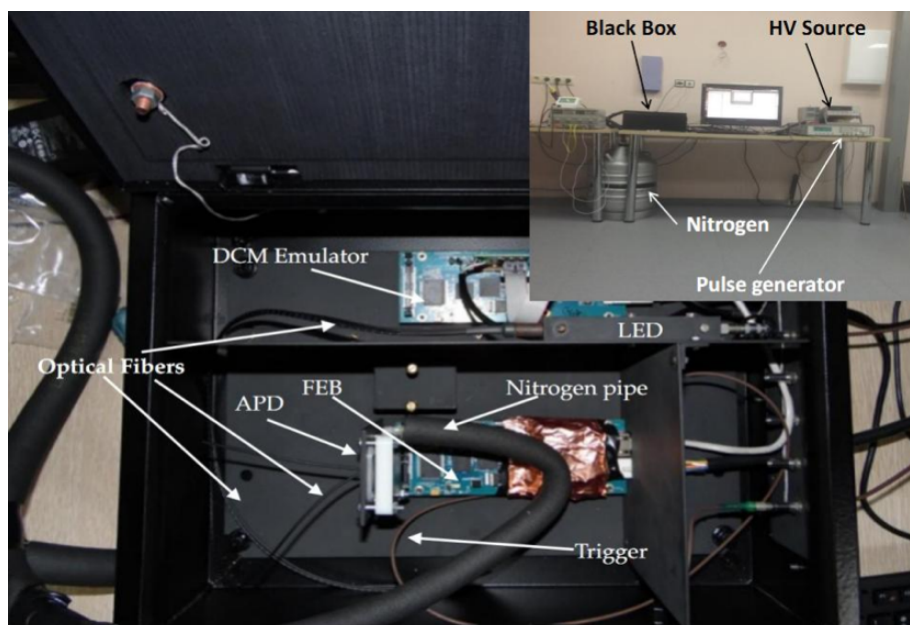
Figure 35. NOvA test bench.

First is the native NOvA electronics – Avalanche PhotoDiode and Front-End Board. Second is the special hardware – download cable, DCM-emulator, LED, Low and High Voltage Sources, Pulse generator and cooling system. Third is a PC with the necessary software. All sensitive devices were placed into a black metal box. The black box allows one to perform all of the measurements with photodetectors, like APDs and PMTs, and screens all external electromagnetic noise. Because APDs in NOvA operate at -15° C we employed a cooling system based on Nitrogen evaporation flow. A pulse generator waits for the FEB trigger and sends the electric pulse to the LED. Then the light pulse from the LED travels through the fibers to the APD, and the FEB reads the data.

Indeed, several important measurements were performed at the JINR NOvA electronics test bench, and more are planned.

4.2.1. Flashes

An important characteristic of the electronics operation is a cross-talk between different channels. It can have several sources and should be adequately understood and described in the Monte Carlo simulation and calibration.

In the Figure 36 an event display in the NOvA FD is presented. One may notice some strange hit structures, which are called Flashes. The main feature of flashes is that sometimes the FEB channels in the same FEB produce signals over threshold simultaneously, but these events take place only if the primary signal is of very high amplitude. Understanding this effect is important for events with high-energy depositions, in particular, for the estimation of Cosmic Ray background and searches for Exotics.
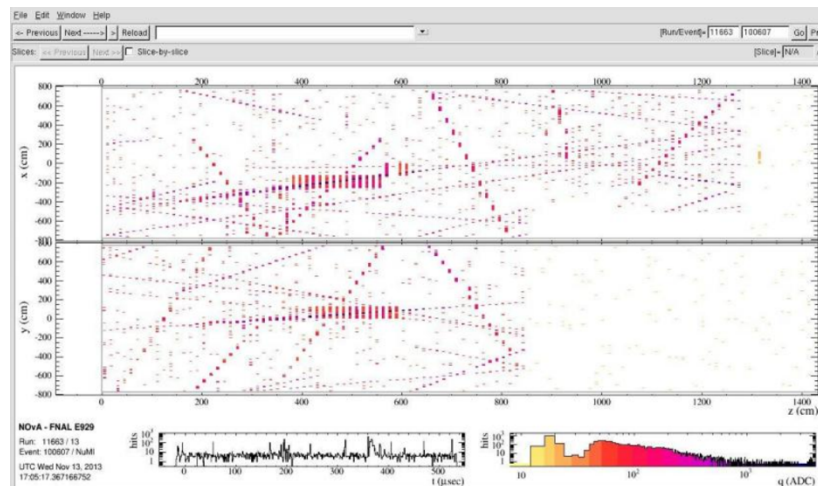
Figure 36. An example of event in Far Detector with Flash.

After building the test bench we began studying the APD response to different light intensities. It was very important for understanding the detectors performance for high energy dissipations.

By sending very high intensity light into a single APD pixel, which saturates the ADC, we found that the same small inverted signals occur in most of the channels within the same FEB (flash-effect). But while checking the FEB by injecting a huge charge into a single FEB channel we observed only normal cross-talk in neighboring channels that drops exponentially.

The next step was to check the APD feeding chain. In the NOvA detectors all APDs operate with a gain of about 100. We also performed a measurement of APD gain with different temperatures to study APD operation voltage at different temperatures (see Figure 37 - left).
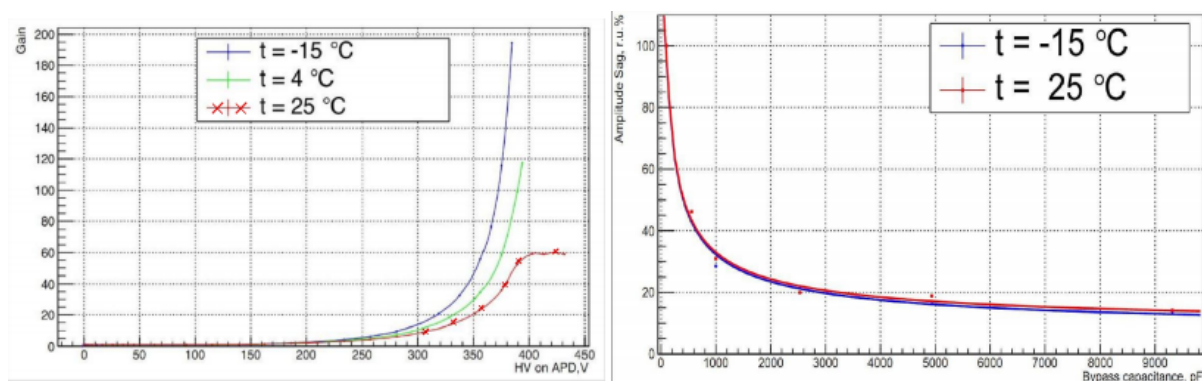
Figure 37. APD gain vs applied voltage with different temperatures (left). APD Sag dependence with respect to the primary effect vs bypass capacitance (right).

We tested different capacitance in the APD bias voltage chain and observed a change in the value of negative cross-talk pulse. It was suggested that the capacitance blocks a voltage drop, which was named the Sag-effect. The Sag was defined as a value of the amplitude of the inverted signal in the neighboring channels in the case of a huge amplitude in the primary one. We applied different amplitudes to the APD and measured the value of the Sag. The result was that the relative value of the Sag does not depend on the amplitude, and is equal to 1.89% for original electronic circuit. The Sag does not depend on the temperature as well. It is the capacitance, which essentially drives the effect (see the right part in Figure 37). As an example, a replacement of the original 100 pF capacitor by a 9.4 nF one reduces the effect sevenfold.

After these measurements, which clarified the situation, the NOvA collaboration has adopted Sag as useful option for dynamic range extension of electronics. In a case where the primary signal saturates a readout channel, the Sag amplitudes travel to the next channels, which are almost free of signals because of low event rate. And, finally, the primary signal's amplitude can be evaluated by many (up to 31) neighboring amplitudes. As a result we can still estimate the primary signal with a reasonable precision. For more information about the results of the test bench activity see [7].

4.2.2. Response to the long signal

An experimental setup was made to study the response of the electronics to long signals. In addition to the ordinary setup, a PMT and a stand-alone ADC were introduced. The PMT was used to monitor the shape of the initial light pulse and ADC with fast sampling to digitize PMT signals. The main idea was to send light with the same integral intensity, which corresponds to a constant charge. We also tried to generate rectangular-like light pulses. The ASIC shaper integrates the APD pulse width and converts it into a rise time, and shaping parameters vary on pulse amplitude (Figures 38, 39).
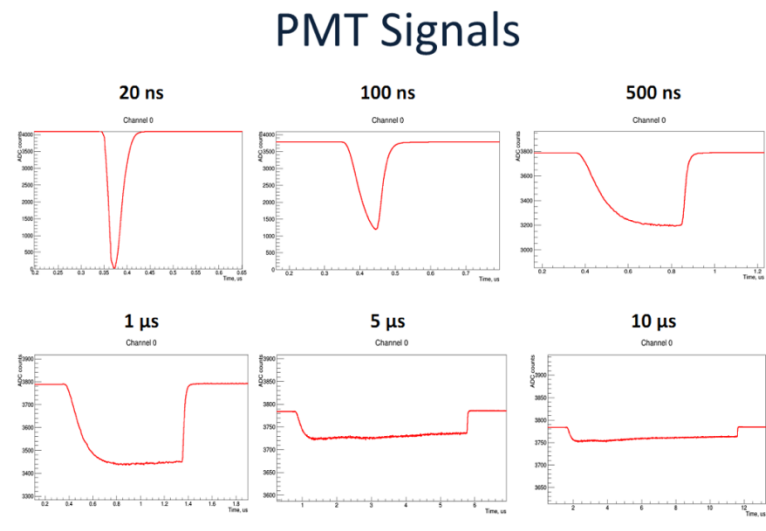
Figure 38. PMT signals on stand-alone ADC.

APD Signals
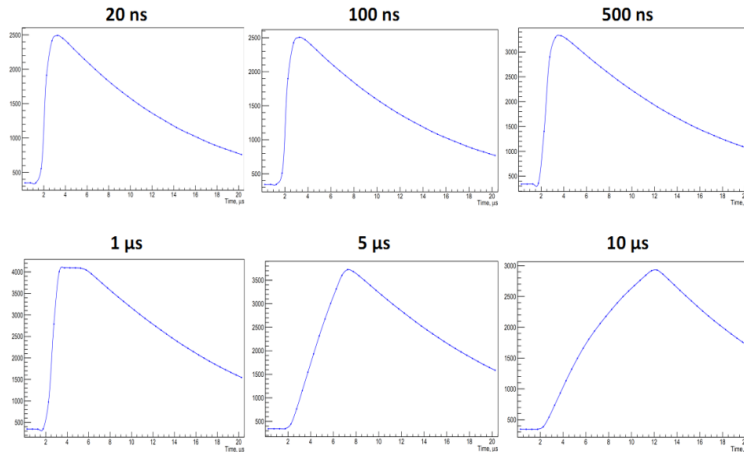
Figure 39. APD signals on the NOvA electronics.

4.2.3. Shaping parameters

For simulation of the detectors' performance a request came from the NOvA collaboration to find precisely all the shaping parameters for both detectors. It was important for computer modeling and Monte-Carlo simulations. The scheme of the measurement was the same that aforementioned. The fall time was found to depend linearly on the amplitude (see Figures 40, 41) and the rise time variation with amplitude was found to be negligible.
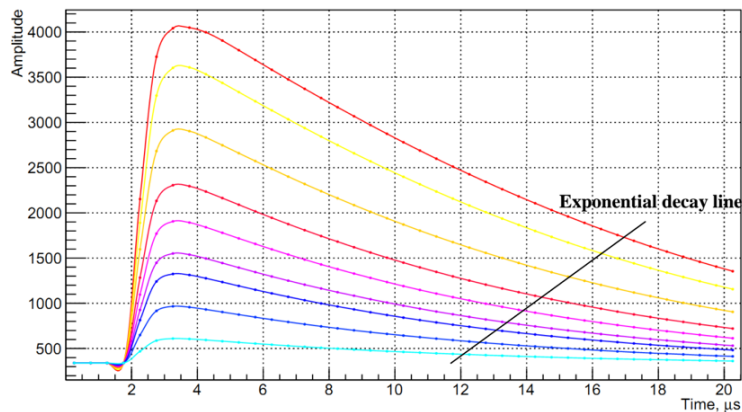
Figure 40. APD signals with different amplitudes.

Fall time vs Amplitude
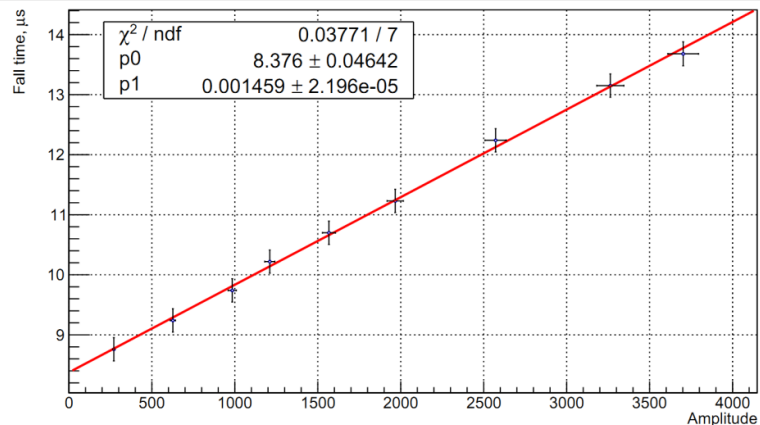
Figure 41. Fall time dependence on the amplitude of the signal.

4.2.4. Future plans

We have developed a powerful tool for the direct manipulation and measurement of native NOvA electronics. Many issues have been studied and we plan to use this test bench also in future.

In addition, we are planning to construct a special setup for measurement of the NOvA scintillator. The NOvA detector is using genuine mineral oil with scintillating dopants. Oil and dopants have been optimized in many parameters: the scintillation efficiency, transparency, light output, etc. However, the effects of quenching for different densities of ionization were not studied experimentally. Knowledge of the Birks coefficients might significantly improve the modeling of energy loss in the detector for a more accurate reconstruction of the neutrino energy.

One of the leading channels of neutrino interaction is the interaction with emission of a proton. Knowledge of the scintillator response to low energy protons is considered by the collaboration as one of the more important tasks.

We are going to make a study of the quenching factor for the NOvA scintillator using alpha and gamma radioactive sources, and cosmic muons as well. We will then test the response of the scintillator on recoil protons by using neutron-proton scattering from a monoenergetic neutron source, ING-27, with an energy of 14.1 MeV. An approximate scheme of measurements is shown in the Figure 42. All of the equipment will be placed in a light-tight black box.
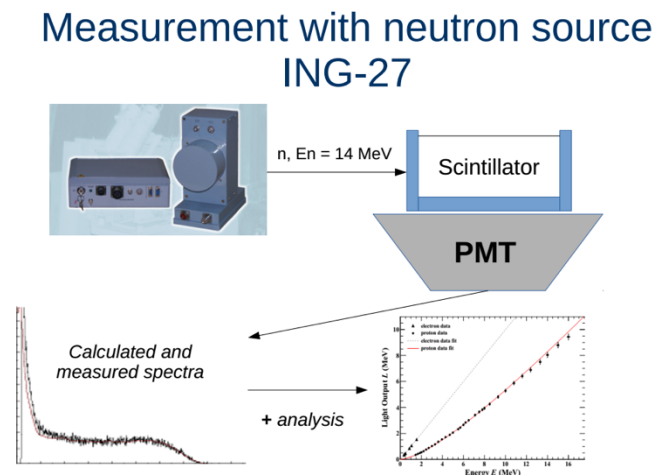
Figure 42. Approximate scheme of the measurement with ING-27.

We also plan to explore the use of the scintillator for particle identification by pulse shape, which is known as gamma/neutron discrimination. The development of a such methodology will further allow for the study of other types of scintillating materials for different experimental and application purposes.

4.3. Computing Infrastructure and Software Development

NOvA is a large-scale neutrino experiment, and it needs a huge amount of computing resources to process all of its data it requires almost a million CPUh per week in its peak. NOvA gets part of its computing resources from the local FNAL computing infrastructure, Fermigrid, from Open Science Grid (OSG). Taking into account the amount of computing resources consumed by the experiment it is obvious that any additional contribution would be very beneficial. As a part of JINR's participation in the experiment we began working on contributing to the experiment's computing resources.

All of the computing resources are located at the Laboratory of Information Technology (LIT). It has different computing facilities: a Tier-1 cluster, combined Tier-2 and local batch-processing cluster, hybrid cluster - HybriLIT - that comprises Graphical Processing Units (GPUs) and coprocessors as well as ordinary CPUs; cloud infrastructure. The Tier-1 cluster cannot be used by NOvA because it is fully dedicated to CMS and NICA. We also decided not to use HybriLIT cluster because NOvA software isn't well-suited to work with GPUs. The rest - Tier-2 cluster and the JINR Cloud - were set up for neutrino event modeling, supporting experimental data acquisition and control, and performing physical analysis.

As a first step we prepared virtual machine (VM) images containing all of the necessary NOvA software to perform physical analysis, combined with the centralized JINR authentication system based on Kerberos. The VMs deployed from these images (or as we call it - iVMs, for interactive VMs) in the JINR cloud are used on a group and personal basis by the local JINR NOvA members, and allow one to work locally in interactive mode or to submit Grid-jobs (a list of which is shown in Figure 43).

Figure 43. Status on VMs by nova users in JINR.

Specially for the NOvA experiment 9 new servers in two different configurations were purchased:
  • Dell PowerEdge R430 2xE5-2650v3, 6x8GB, 2x2TB NL SAS - 5 servers;
  • Dell PowerEdge R430 2xE5-2650v3, 6x16GB, 4x4TB NL SAS - 4 servers.

These servers were used to expand the JINR Cloud's capacity and became the basis for the virtual batch cluster and a Grid-site that process jobs from both local JINR NOvA team and NOvA-jobs coming from OSG, contributing directly to the NOvA collaboration. In this system every component of a Grid-site is virtualized, which is a first-time experience for the JINR Grid-sites and is an important step for further development of computing models at JINR.

The virtual Grid-site (see Figure 44) consists of Computing Element (CE) and a batch-system. The HTCondor batch-system was used to handle worker-nodes and distribution of jobs across them, and HTCondor-CE - a modified version of HTCondor - as a CE playing the role of a

gatekeeper that handles authentication and translates jobs coming from the Grid-environment into the local batch-system's format.
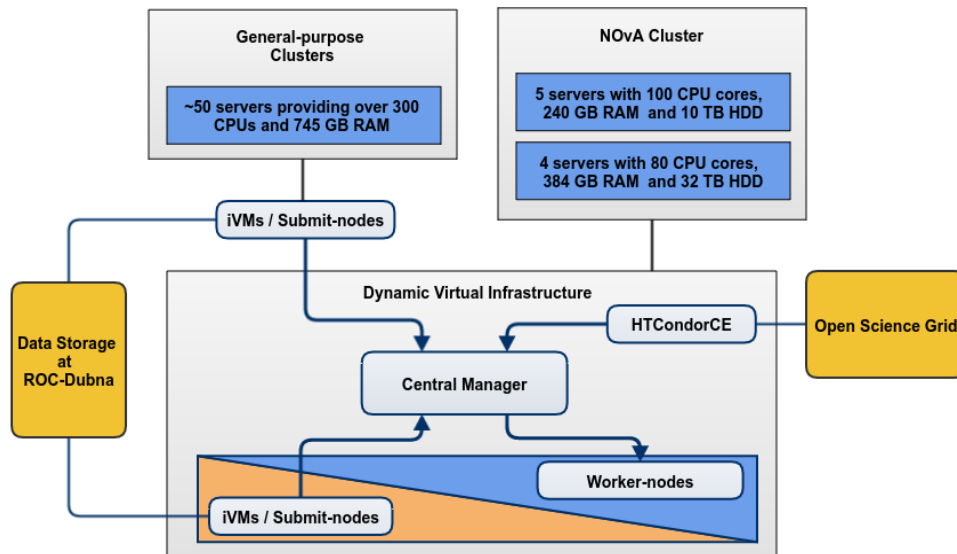
Figure 44. The scheme of the cloud infrastructure.

Building the system in the cloud gave us a possibility to dynamically scale the batch-cluster to add up opportunistic resources to the batch-system or to give out some resources to supplement general-use virtual machines in accordance with current needs and workload.

Since the time of the commissioning of the system it has proven to be useful, and has made a significant computing contribution into the experiment. The statistics are shown in Figure 45.
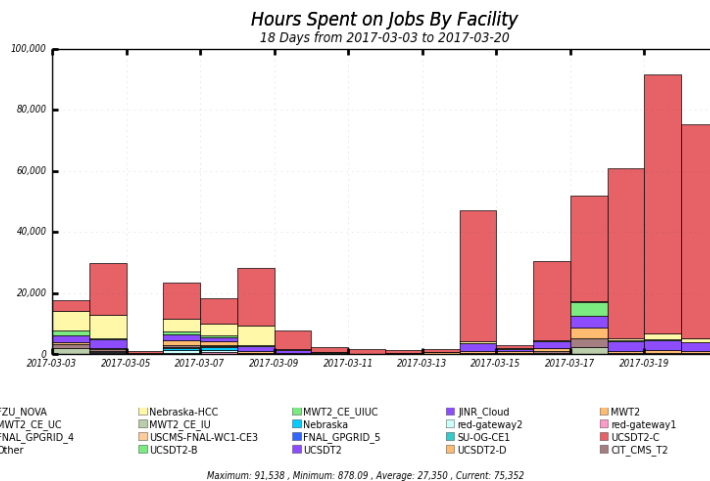
Figure 45. CPU hours statistics spent by Institutions computer farms in March during 2 weeks.

Independently of preparing cloud resources for NOvA, JINR Tier-2 site was successfully integrated into OSG and is also contributing to NOvA at scales comparable to the virtual Grid-site deployed in the JINR Cloud.

Despite all of the success, further efficient extension of the computing infrastructure dedicated to NOvA, and therefore increase of its contribution to the experiment, requires the deployment of data-caching mechanisms and, probably, a dedicated Storage Element (SE) to decrease the usage of expensive and limited data transfer channels.

4.4. Data Analyses

4.4.1. Monte Carlo tuning

The simulation of neutrino interactions starts with modeling of the hadron production within the target, focusing in the horns, and downstream tertiary production to determine the production rate and energy spectrum of each neutrino flavor from the decay of pions, kaons, and muons in the decay pipe using the FLUKA simulation package [6,7] and the FLUGG GEANT4 geometry interface [10]. The resulting simulated neutrinos are stored in flux files along with information about their parentage, and they are used as inputs to the neutrino event generation stage performed with GENIE [11]. Factorizing out the simulation of the neutrino flux from the rest of the simulation minimizes the number of times this computationally intensive step needs to be run, as well as allowing for after-the-fact tunings of hadron production or focusing parameters. Becausethe far detector is located on the surface, cosmic rays are a significant background; we generate cosmic ray events with CRY [12]. The particle lists generated by either GENIE or CRY are then passed to GEANT4 [13,14], which propagates particles through the detector and produces energy deposits in active material. Finally, the list of energy deposits in active material are passed to a parameterized front-end simulation which converts energy deposits into scintillation light, transports scintillation light to the APD, and simulates the readout electronics response. The final output is formatted like raw data.

For the recent analysis [3,4], neutrino interactions were modeled using GENIE 2.10.2 (for the first analysis [5, 6], the version 2.8.0i was used). Evidence presented by other experiments suggests an additional event rate and an alteration of kinematic distributions arising in neutrino scattering on nuclei. Analysis of the hadronic energy distribution in the NOvA ND data further supports this conclusion. While this is an area of active theoretical development, for the current NOvA results our simulation has been augmented with a semi-empirical model in GENIE that posits neutrinos scatter from nucleon pairs (np and nn) within the nucleus. The model is inspired by observations of rate enhancements in electron-nucleus scattering data and their treatment via 2-particle 2-hole (2p2h) calculations that include meson exchange currents (MEC). Adjustments were made to the semi-empirical model to achieve a more constant cross section for 2p2h-MEC processes above 1 GeV. These events are also reweighted as a function of three-momentum transfer and visible hadronic energy to match the ND data. The addition of 2p2h-MEC processes increases the simulated event rate by about 10% in both detectors, but the mean reconstructed neutrino energy and spectral shape remains largely unchanged. Additionally, as suggested by a reanalysis of bubble chamber data, the rate of ν_μ-CC non-resonant single pion production in GENIE is reduced by 50%.

The JINR group is working on several parts of the simulation in the NOvA experiment: neutrino-nucleon cross sections, electronics readout, supernova fluxes and cosmic ray muons.

Neutrino-nucleus cross sections are important for neutrino oscillation experiments to calculate event rates and energy distributions in both near and far detectors. Cross section measurements, which are used to develop and tune neutrino-nucleus interaction models, currently have 10-50% uncertainties depending on the process.

One of the most significant uncertainties affecting the reliability of extraction of the neutrino mixing parameters from the data of experiments with atmospheric and accelerator (anti)neutrino beams is the huge uncertainty of the axial-vector and pseudo-scalar form factors of the nucleon. Within the conventional dipole parametrization for the axial form factor M_A we can not describe the latest and most reliable experimental data for both low and high energy regions, e.g., MiniBooNE and NOMAD experiments, at the same time.

The BLTP neutrino group developed a phenomenological method based on the notion of the so-called "running axial mass", which permits a high-accuracy calculation of the total and differential QE cross sections for all nuclear targets, and at all energies of interest, by utilizing the conventional RFG model [15,16].

Within the NOvA project at JINR the "running axial mass" approach was developed and implemented into the latest version of GENIE. This option was presented at NOvA collaboration meetings and was considered as a valid model to generate neutrino-nucleon interactions. We are planning to implement this method in the full data tuning and processing chain of the NOvA experiment and use it for both modeling and interpretation of the data in the near and far detectors, decreasing existing systematic cross section uncertainties.

4.4.2. ν_e Analysis Optimization

One of the responsibilities of JINR in the ν_e analysis group is the optimization of the analysis and, in particular, neutrino and antineutrino cut tuning.

The NOvA analyses are constantly developing. Among the most significant recent updates was implementation of the Convolutional Visual Network (CVN) algorithm described above in the ν_e analysis section.

CVN implementation into the NOvA analysis has made big progress: in terms of experiment "exposure" CVN gives +30% in comparison with more traditional event classificators. It produces a 76% pure sample of electron neutrino CC events. The most efficiency it shows itself in rejecting NC and cosmic background. All these factors made CVN the main event classifier.

The next step in further improving this tool will be in training it to identify not only interaction types but also the particles which were produced.
One of the closest improvements of upcoming analyses will be in retuning cuts for neutrino and antineutrino modes. Currently NOvA is running in antineutrino mode. This means that the 2018 analysis will be for the first time in NOvA made with antineutrinos. However, analysis cuts have not yet been tuned for antineutrinos. And this work deserves our careful attention.

The situation in neutrino analysis is much better, but still not perfect. Current neutrino selection criteria were initially optimized before the first analysis in 2015. The cosmic event rejection was optimized before the second analysis. But the overall effect of cuts was not tuned. Moreover, the strategy of analysis suggests looser cuts for the future. All these factors make the cut-tuning task one of the most significant improvements for future analysis.

Possible improvements for the neutrino cut tuning are: loosening of Data Quality cuts, Preselection (Energy, Number of Hits and Length of Shower), keeping events with all Pt/P, analysis with 4 PID bins instead of 3, and keeping uncontained events in data sample. According to preliminary estimations all these improvements give >+20% in exposure. This is as significant as was the implementation of CVN.

One more possible avenue for nue analysis is the application of the BDT algorithm from numu analysis to nue. The cosmic rejection power of NOvA BDT is a well known fact. But incorporating it into analysis require many tests. So, BDT implementation is one of the possible future analysis upgrades after this year's analysis.

4.4.3. Detection of core-collapse Supernova neutrino signal

4.4.3.1 Supernova neutrino signal
Core-collapse supernovae produce about 10^{58} neutrinos during the first seconds after the explosion. These neutrinos, carrying about 99% of the initial gravitational energy of the collapse, play a crucial role in the explosion mechanism (see Figure 46).
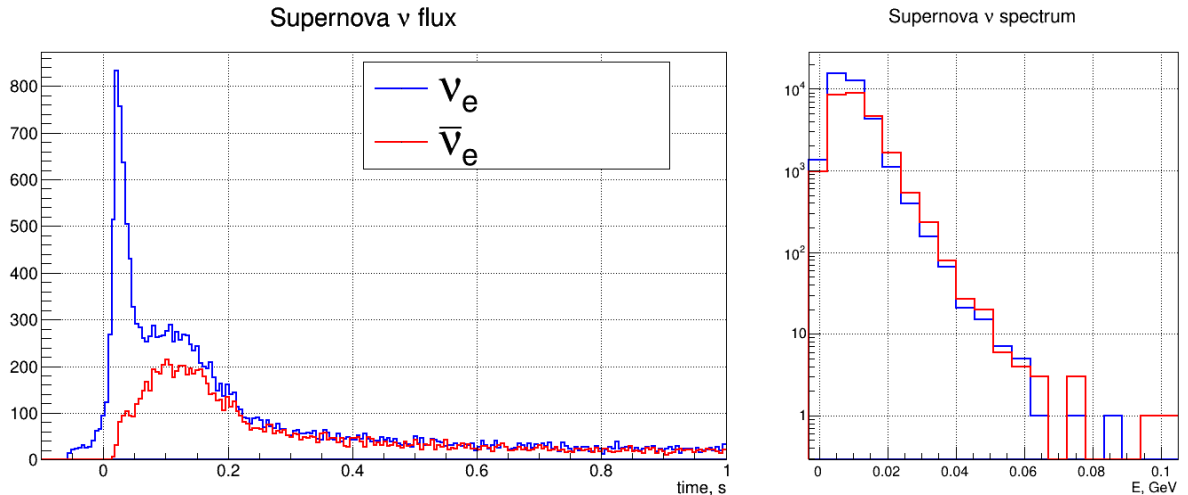
Figure 46. Neutrino composition and spectra from supernova explosion.

During the neutronization process in the stellar core, a burst of electron neutrinos is produced within the first 10 milliseconds. Due to the enormous neutrino density their interaction with the collapsing matter produces a shockwave breakout, and thus triggers the supernova explosion. This process is accompanied by the emission of all other flavours of (anti)neutrinos.

Existing models of core-collapse supernova explosions feature complex 3D simulations of the processes during the core collapse. Results of these simulations predict various neutrino spectra and energy luminance curve vs. time for different models.

4.4.3.2. Supernova signal simulation
A dedicated simulation package was developed to simulate interactions of supernova neutrinos inside the NOvA detectors.

This package interfaces several models of supernova neutrino fluence with the GENIE neutrino interactions generator [11], which is used in the NOvA simulation for other analyses. This allows easy integration with the default NOvA simulation pipeline.

One of the features of the developed package is the possibility to simulate the time structure of the supernova neutrino signal, which is important for the development of real-time triggers. For this study we consider only the processes of inverse beta decay and elastic neutrino scattering on electrons.

We plan to include other processes to increase our sensitivity.

4.4.3.3. Candidate selection procedure
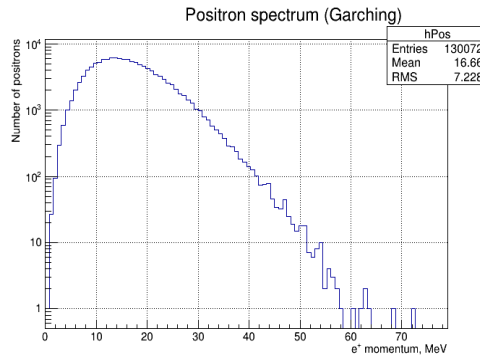
Figure 47. Positron spectrum from supernova IBD interactions

We are considering the positron from the IBD process (see Figure 47) as our main signature for interaction candidate.

A positron with 10-30 MeV energies typically produces hits in 1-3 scintillator cells in the NOvA Far Detector. Detecting such a weak signal in the detector, designed for 2 GeV neutrino beam, can be challenging.

4.4.3.4. Background sources and rejection

Since the Far Detector is located on the surface and has very small overburden, it is exposed to the atmospheric cosmogenic background: muons and atmospheric showers. In our analysis muon tracks are reconstructed using Hough transformation tracking algorithm, so we discard the hits along these tracks and in the proximity to the track ends, to reject Michel electrons. The high-energy showers are tagged by detecting a short peak in the timing distribution.

The noisy electronic channels produce a lot of single hits. Also, the channels within one DCM (32 channels in one plane) can produce correlated noise, producing multi-hit clusters. We can reject most of this background, selecting only the candidate clusters with hits in both X and Y views, i.e. in different planes.

Masking the channels with the highest activity with the channel map does additional rejection of electronic noise. Finally, we apply cut on the sum of cluster hits' amplitude (ADC).

4.4.3.5. Positron detection efficiency
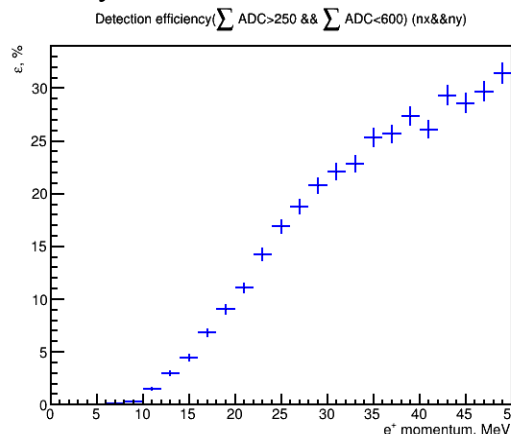
Figure 48. Efficiency of positron detection depending on positron momentum (right).

Applying the described selection procedure, we can estimate the detection efficiency using a simulated sample of positrons, uniformly distributed within the detector and with uniform direction (see Figure 48).

4.4.3.6. Data driven triggering in NOvA

NOvA utilizes the data-driven trigger (DDT) system to perform the data reconstruction online and to decide which time range of data should be saved for further offline analysis.

To achieve this, the data stream from the detector is sliced in 5ms blocks (called milliblocks), which are then distributed to more than 80 buffer nodes.

Each node stores the milliblock in the ring buffer, so this data can be retrieved by request until the buffer is rotated. Currently the buffer depth allows us to store data for about 10 minutes.

At the same time the buffer node processes the milliblock, applying the basic reconstruction and analysis. If this block satisfies trigger conditions, the triggering signal is sent to the central Global Trigger node, which then requests the data from buffer nodes and saves it to the permanent storage.

4.4.3.7. Supernova trigger infrastructure

In contrast to other triggers, where the trigger decision can be made based on 5ms data slice, supernova neutrino signal lasts for several seconds. This means that we must process several hundreds of milliblocks in parallel on many buffer nodes, and then accumulate the results and make a trigger decision.

The scheme of the supernova trigger system is presented in the Figure 49.
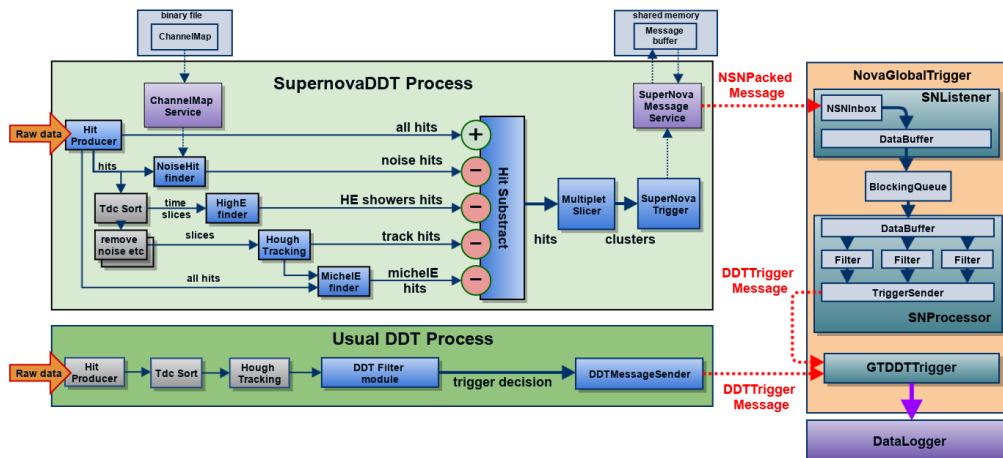
Figure 49. Scheme of Supernova DDT process in comparison with usual DDT trigger.

Each DDT process performs the interaction candidates' selection, described in the previous section, within a 5ms milliblock, and then sends the number of candidates to the GlobalTrigger node.

The GlobalTrigger application receives this data and sorts it into a time sequence. Then this timed sequence is convolved with the filtering kernel to suppress the background fluctuation and enhance the statistical significance of the signal (see Figure 50).
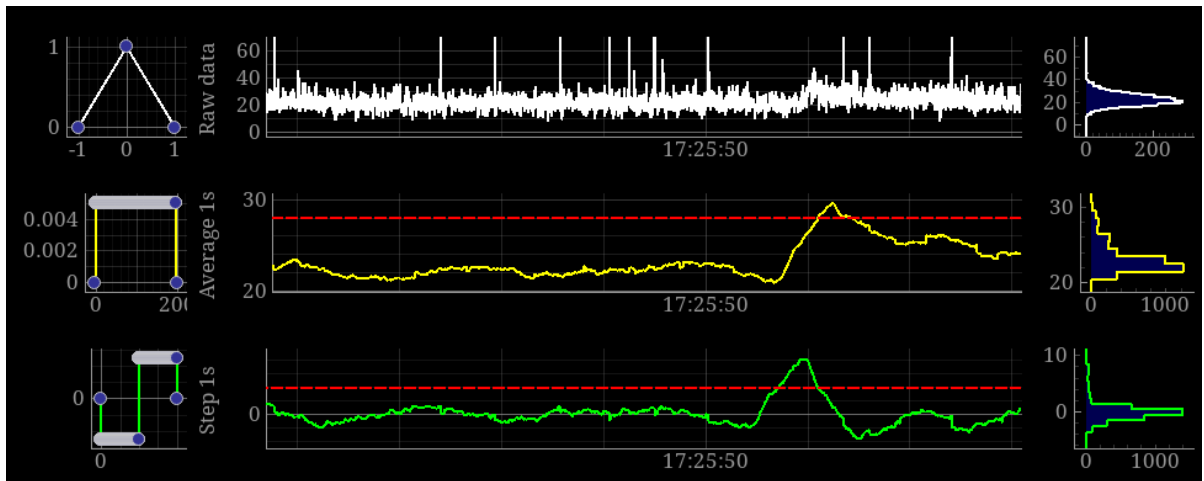
Figure 50. Example of supernova signal detection using filters to enhance the signal.

4.4.3.8. Supernova detection efficiency

The developed candidate selection procedure allows for the evaluation of the probability to detect a supernova depending on the distance to the progenitor star. We assume that the number of observed background and signal interaction candidates during the first second of a supernova follows the Poisson distribution.
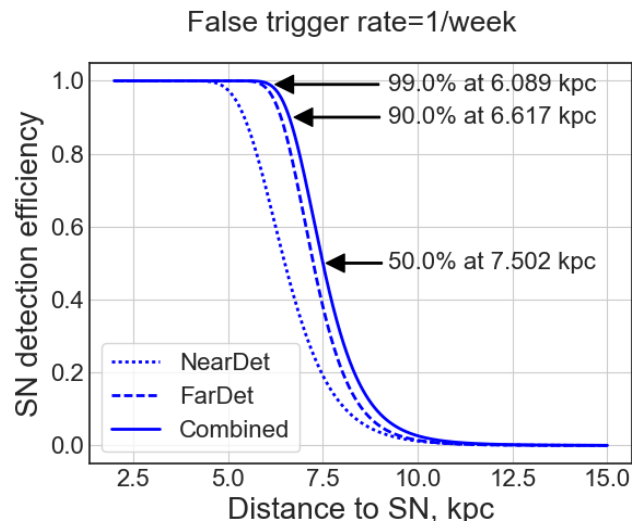
Figure 51. Supernova detection efficiency on a distance from supernova explosion.
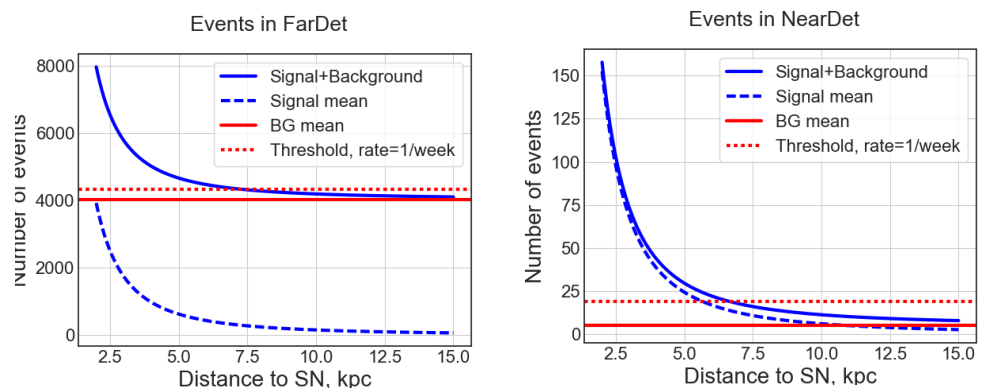
Figure 52. Event rates for signal and background.

This sensitivity can be improved if we include additional interaction channels, optimize the selection criteria maximizing the statistical significance, and also use the single hits from near detector.

4.4.4. NOvA as a Cosmic-Ray Telescope

Since the Far Detector of the NOvA experiment is located on the surface and has a huge size, it can be considered one of the biggest scintillator cosmic-ray telescopes. The number of cosmic rays passing through the Far Detector per second is of the order of 10^5 (see Figure 53).
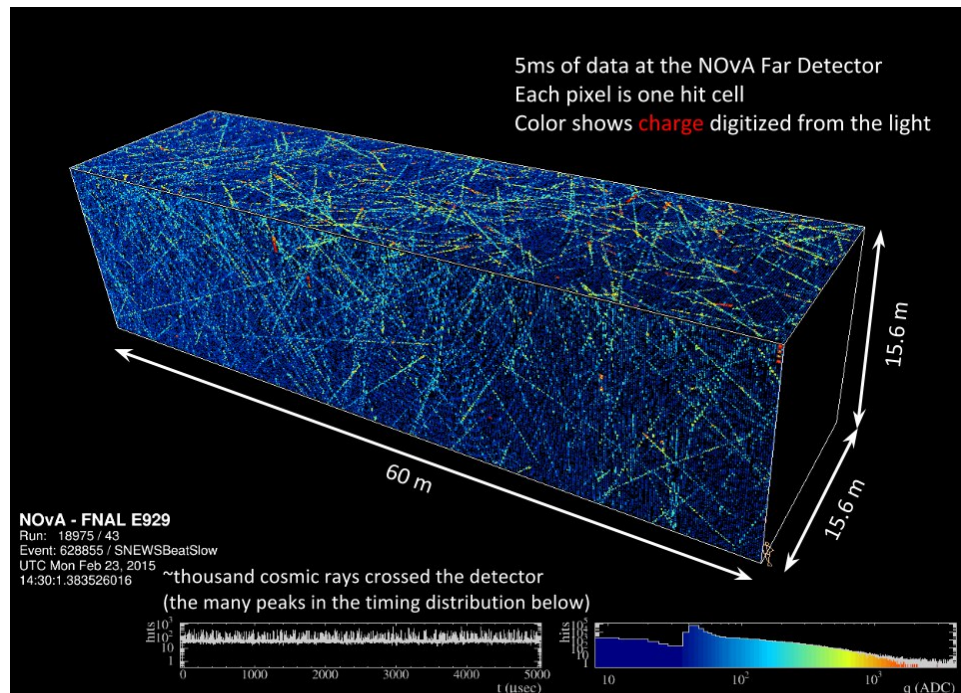
Figure 53. Event display of NOvA Far Detector with many cosmic ray tracks.

Muons constitute one of the main portions of secondary cosmic rays. There are several interesting phenomena, connected to cosmic-ray muons, which could be studied with Far Detector of NOvA, including the following. A huge influx of cosmic ray events allows us to study the east-west asymmetry of cosmic ray muons. Due to the large statistics available, very high-energy muon events can be observed in the Far Detector. Also, thanks to the size of the detector, one can observe events with high multiplicity parallel cosmic muons from Extensive Air Showers in the NOvA Far Detector.

4.4.4.1. East-west asymmetry

JINR participates in cosmic-ray studies of the NOvA collaboration, in part dealing with the cosmic muon east-west asymmetry. Measurement of the east-west asymmetry of cosmic muons can help with discrimination of the primary cosmic ray mass composition [17].

The phenomenon is based on the Lorentz force, that incline charged particles, moving in geomagnetic field. In the Northern Hemisphere for the particles coming to a certain point on the Earth from the east, some of the trajectories are forbidden, and cosmic ray flux from east is smaller than from the west (see Figure 54).
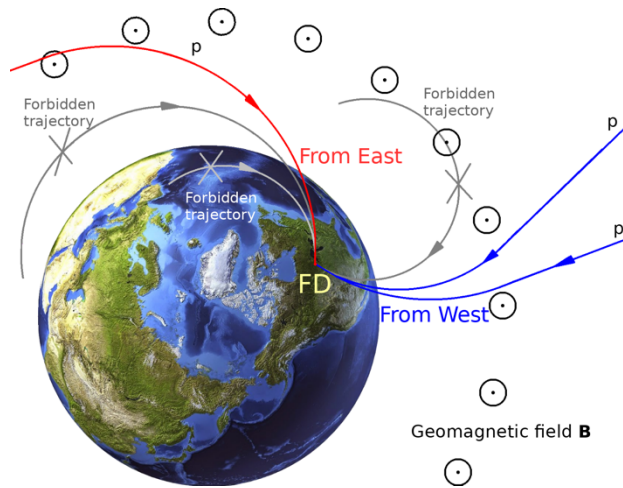
Figure 54. East-west asymmetry of cosmic rays for NOvA FD.

The study of east-west asymmetry in the Far Detector of NOvA is complicated by the fact that the overburden covering the detector and the rock surrounding it are also asymmetrical (see Figure 55, 56).
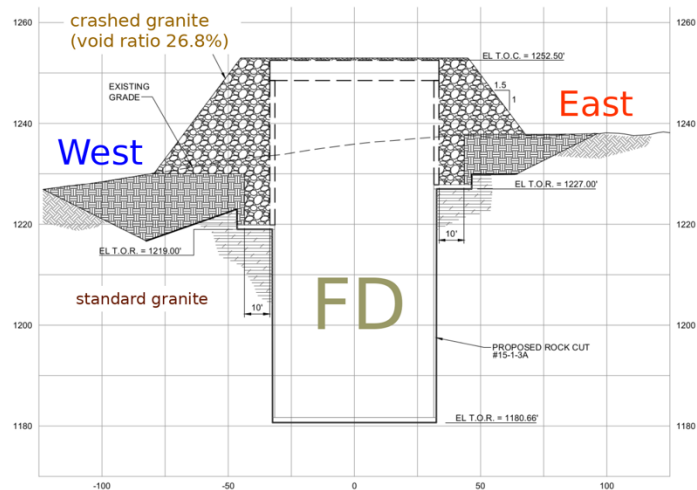
Figure 55. Asymmetry of the hill around Far Detector.

When corresponding corrections are applied, we will obtain the east-west asymmetry measurement at the NOvA Far Detector coordinates and improve the knowledge about the geomagnetic field and primary cosmic rays.

39
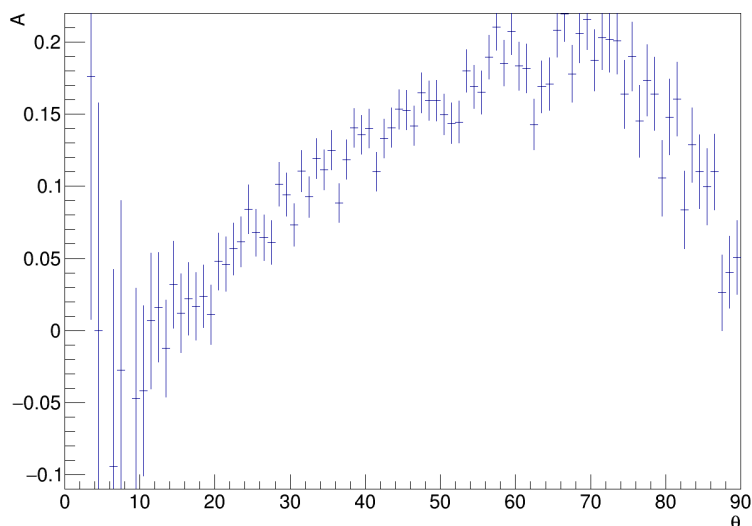
Figure 56. East-west asymmetry of cosmic-ray muons, stopped in the Far Detector of NOvA, without hill asymmetry correction. Asymmetry is defined as *A=(W-E)/(W+E)*, where *W* is cosmic muon flux coming from west, *E* is one from east.

4.4.4.2. High-energy cosmic-ray muons

Another study is dedicated to the observation of very high-energy cosmic-ray muons and the measurement of their energy. The fact is that analysis of muons with the energies of ≥100 GeV, produced in the upper atmosphere, can provide information about the spectrum and composition of primary cosmic rays and the details of the interaction of hadrons with nuclei at energies inaccessible to current accelerators.

It is possible to estimate the energy spectrum of these high-energy muons using the method suggested in [18]. It is one of the methods of muon energy reconstruction, based on measuring the specific components of energy loss (see Figure 57).

In general, the main processes of high-energy muon interaction, leading to the formation of secondary cascade showers in matter, are:
  - bremsstrahlung,
  - direct electron-positron-pair creation,
  - delta-electron formation,
  - inelastic interaction of muons with nuclei.
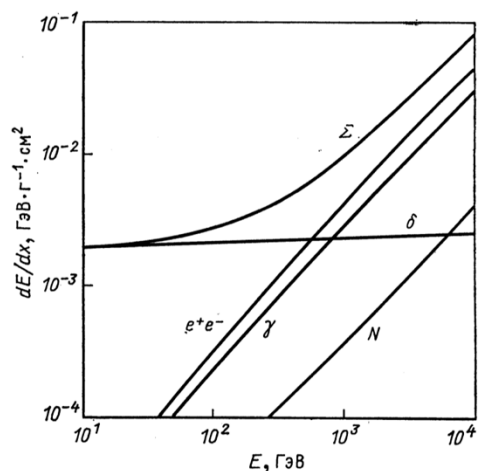
Figure 57. Energy loss components of muon (in iron). This picture is borrowed from [18].

Muon energy loss can be defined as $-(dE/dx)=a+bE$, where a is the ionisation energy (δ-electrons) loss and bE is the sum of e-pair production, bremsstrahlung, and photonuclear contributions (a and b are slowly varying function of the muon energy) [19]. At $E>1$ TeV energy loss is almost proportional to E.

The key point of the implementation of this method is the separation of relatively mild fluctuating loss on the e-pair formation and catastrophic collisions in the processes of bremsstrahlung and nuclear interactions. When we manage this, we will be able to estimate the muon energy from its energy loss.
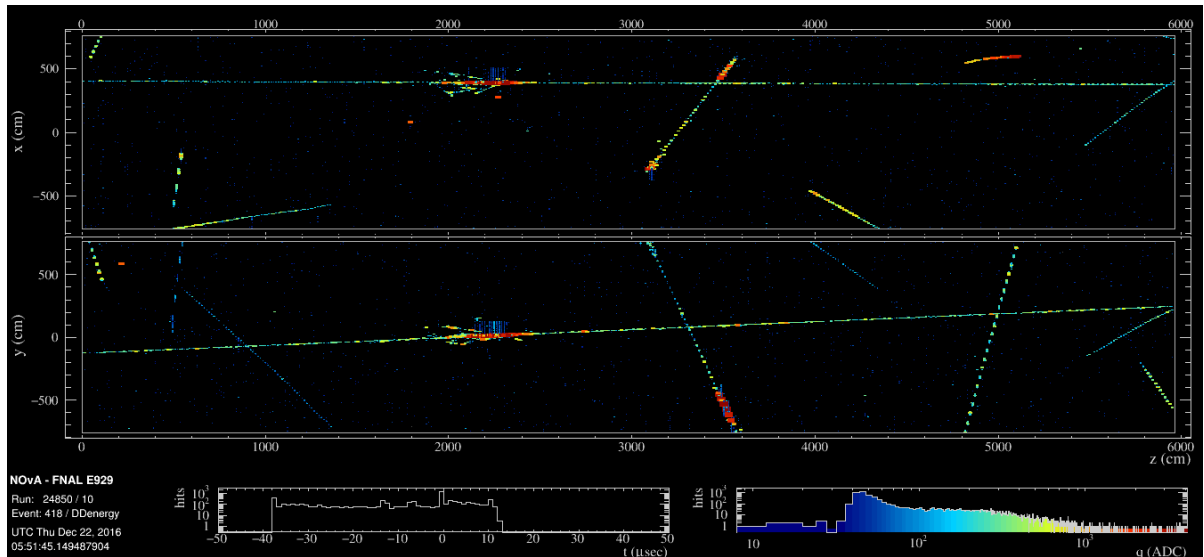
Figure 58. High-energy muon in real data of the Far Detector of NOvA.

4.4.5. Slow Monopole Detection

The NOvA far detector is well suited to the search for exotic particles due to its technical opportunities. One example of these exotic particles are the "slow" magnetic monopoles. A measurement of the expected signals from the monopoles has been performed on the NOvA test bench at JINR . It has been proposed to develop the signal simulation of the "slow" mode (the slow monopoles velocity is $\sim 10^{-3}$ times the speed of light) in comparison with the typical signals due to elementary particles. It is assumed that the energy deposition of such monopoles should be sufficiently large. As a whole it promotes searches or it can limit the existence of monopoles in a wide range of parameters, previously unreachable in other experiments (MACRO, SLIM, RICE, IceCube).

Quantum mechanical formulation of the magnetic monopoles was made by Paul Dirac in 1931. Searches for these particles are very important for several reasons:
1. Their existence would explain the quantization of electric charge.
2. It is possible to restore symmetry between electricity and magnetism by means their introduction into the theory of electromagnetism.
3. Magnetic monopoles naturally appear in Grand Unification Theories (GUT).

The Dirac's electric charge quantization relation says $e \times g = n \times \hbar c/2$, where e is a basic electric charge and n is an integer. This means that magnetic monopoles could have a magnetic charge (g) 68.5 times greater than the charge of the electron. As a result they are expected to be very highly ionizing. "Slow" monopoles with $\beta < 10^{-2}$ can be identified due to their linear tracks with long transit times through the detector. Monopoles with this β take 5μs to cross the entire

detector, in comparison with cosmic muons which take only 50ns. On the left of Figure 59 you can see a simulated monopole and on the right the monopole energy loss.

Figure 59. Simulated monopole in Far Detector (left) and monopole energy loss depending on it's beta (right).

The slow monopole trigger was implemented in June 2015. It allows one to identify slow ($\beta < 10^{-2}$ monopole) tracks by checking the number of plane gaps between the entry and exit hits. We look at all of the hit planes in the contained area and look for gaps.
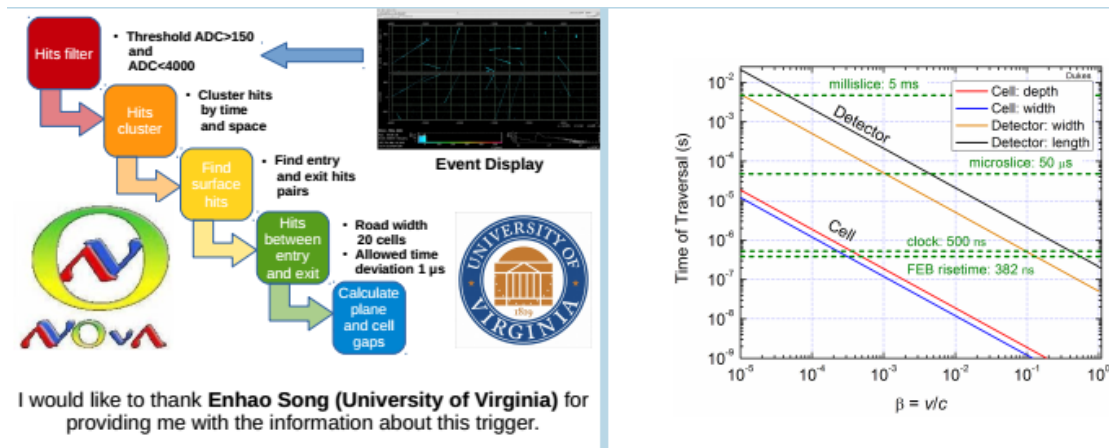
Figure 60. Mechanism of the slow monopole trigger (left) and time of traversal of the monopole through the Far Detector depending on it's beta (right).

We have a special procedure for "catching" a monopole track in the real data:
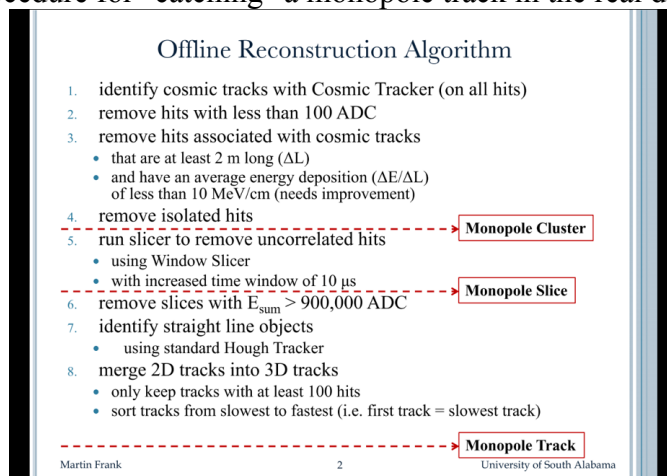
Figure 61. Special offline reconstruction algorithm for monopole event selection.

The NOvA far detector is rather sensitive to lighter monopoles and has the unique potential to "touch" a new region of phase space due to its location on the surface and its large surface area. These factors give us very good chance to "catch" the magnetic monopoles.

4.4.6. Near Detector Measurements

The intensity of neutrinos in the Near Detector is such that multiple neutrino interactions occur in a typical beam spill, Figure 62. This allows NOvA to collect a large dataset of neutrino interactions, which enables for the characterization of the beam content and flux, neutrino interaction physics measurements, comparison of detailed Monte Carlo simulations to physics signals, and the assessment of many key detector systematics.
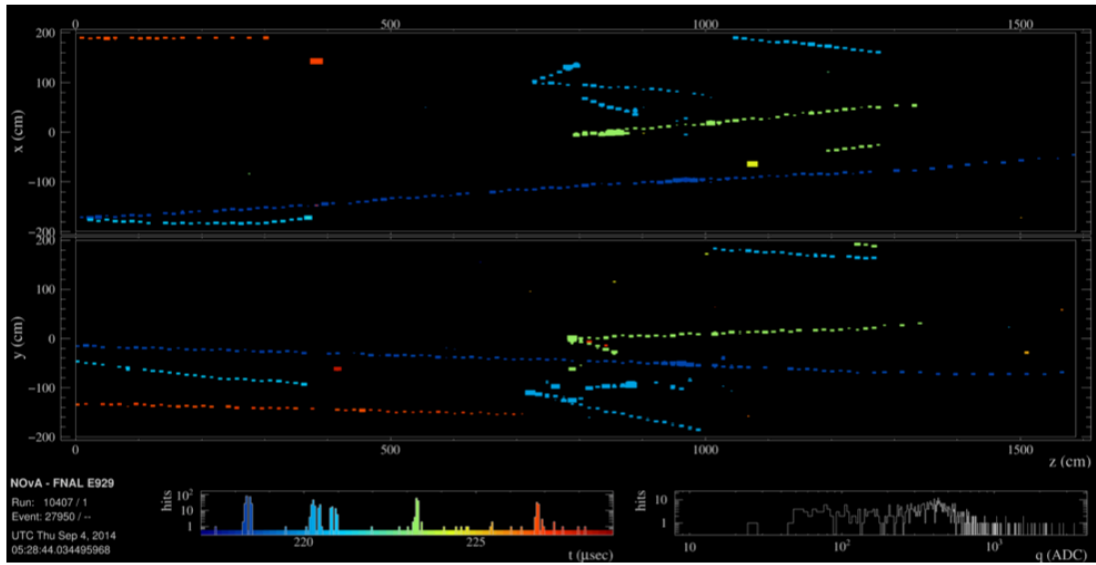
Figure 62. A NOvA Near Detector event with three muon tracks from the rocks and two neutrino interactions, this shows the capabilities of the NOvA Near Detector.

The NOvA ND group has a large-scale program of different physics measurements. In particular, NOvA is working to characterize the muon/electron neutrino charged current interactions on the detectors nuclear materials. The JINR group covers the following activities: single proton production channel, coherent interactions with charged pions, and s-quark production including exotics channel with pentaquarks. Most of these tasks are motivated by the experience gained by the JINR team members from the analysis of the NOMAD data.

5. People and Tasks

#	Name	Laboratory	Tasks	FTE
1	Allakhverdian, Vladimir	DLNP	ND Physics, s-quark prop	0.4
2	Amvrosov, Veniamin	DLNP	Numu oscillation analysis	0.1
3	Anfimov, Nikolay	DLNP	Det operations, test stand	0.3
4	Antoshkin, Alexander	DLNP	Det operations, test stand	0.3
			Exotics, slow monopoles	0.3
			Det control, ROC-liaison	0.1
5	Balashov, Nikita	LIT	Computing	0.3
6	Baranov, Alexander	LIT	Computing, cloud	0.1
7	Bolshakova, Anastasia	DLNP	Reco, proton ID	0.5
			Det sim, ADC thresholds	0.5
8	Bilenky, Samoil	BLTP	Oscillation theory	0.1
9	Dolbilov, Andrey	LIT	Computing, network support	0.1
10	Kakorin, Igor	VLHEP	Det simulation, GENIE	0.5
11	Klimov, Oleg	DLNP	Reco, proton ID	0.6
12	Kolupaeva, Liudmila	DLNP	Nue oscillation analysis	0.8
			Software, release manager	0.2
13	Kullenberg, Christopher	DLNP	ND Physics, coh pion	0.6
14	Kuzmin, Konstantin	BLTP	Det sim, cross sec theory	0.1
15	Kuznetsov, Evgeny	LIT	Computing hardware	0.1
16	Matveev, Victor	BLTP	Theory, Coll management	0.1
17	Morozova, Anna	DLNP	Exotics, CR muons	0.3
18	Naumov, Vadim	BLTP	Osc and cross sec theory	0.3
19	Olshevskiy, Alexander	DLNP	Coll and JINR tasks management, IB-rep	0.5

20	Petrova, Olga	DLNP	Exotics, CR muons	0.7
			Det sim, cross sec calc	0.3
21	Samoylov, Oleg	DLNP	Det sim, co-convener	0.5
			Det control, ROC-manager	0.3
			JINR ana coordinations	0.1
			Coll manag, deputy at JINR	0.1
22	Sheshukov, Andrey	DLNP	DAQ, software dev/support	0.3
			DDT, supernova trigger development	0.3
			Exotics, SN detection	0.3
			Det control, ROC software	0.1
23	Sotnikov, Albert	DLNP	Det operations, test stand	0.1
24	Velikanova, Darya	DLNP	Det operations, test stand	0.1
	TOTAL			**10.3**

The average age of the JINR NOvA team is ~35 years. There are 5 bachelor and master students, 8 young scientists preparing PhD, 4 engineers, 4 staff members with PhD degree and 3 professors.

6. Requested Resources

For the proposed extension of the NOvA project at JINR the following resources are required:

1. 15K$ (5K$/year) - Maintenance of the ROC-Dubna, including satellite internet backup connection, 4G and international telephone line fee, a few monitors and other broken equipment replacements.

2. 15K$ (5K$/year) - Office equipment (aging desktop and laptop computer replacement) for team members.

3. 15K$ (5K$/year) - Additional hardware for tests, including DAQ and analysis computers.

4. 195K$ (65K$/year) - Computing infrastructure extension. We plan to add 5 servers (100 cores, ~50K$) and 100TB disk space (~15K$) per year in order to cope with increasing data and MC volumes and complexity of analysis. After 3 years that will double our computing power with respect to what is available for NOvA at JINR now.

5. 180K$ (60K$/year) - money for visiting FNAL, conferences and meetings elsewhere. This request is 30K$ less than for the previous project, despite the significant increase in JINR involvement and responsibilities in NOvA. This is mainly due to the successful construction of ROC-Dubna at JINR, and the possibility to take NOvA detector shifts locally.

7. References

[1] Feng Peng An et al. (Daya Bay Collaboration), e-Print: arXiv:1610.04802 [hep-ex]

[2] http://www-nova.fnal.gov/nova_cd2_review/tdr_oct_23/tdr.htm

[3][*) P. Adamson et al. (NOvA Collaboration), e-Print: arXiv:1701.05891 [hep-ex]

[4] [*) P. Adamson et al. (NOvA Collaboration), e-Print: arXiv:1703.03328 [hep-ex]

[5] [*) P. Adamson et al. (NOvA Collaboration), Phys.Rev.Lett. 116 (2016) no.15, 151806, e-Print: arXiv: 1601.05022 [hep-ex]

[6] [*) P. Adamson et al. (NOvA Collaboration), Phys.Rev. D93 (2016) no.5, 051104, e-Print: arXiv: 1601.05037[hep-ex]

[7] A.Antoshkin, NOvA internal talk DocDB #14261

[8] T. Bohlen et al., The FLUKA Code: Developments and Challenges for High Energy and Medical Applications, Nucl. Data Sheets 120, 211 (2014).

[9] A. Ferrari, P. R. Sala, A. Fasso, and J. Ranft, FLUKA: A multi-particle transport code (Program version 2005), Technical Report CERN-2005-010 CERN 2005.

[10] M. Campanella, A. Ferrari, P. Sala, and S. Vanini, First Calorimeter Simulation with the FLUGG Prototype, Technical Report CERN-ATL-SOFT-99-004 CERN 1999.

[11] C. Andreopoulos et al., The GENIE Neutrino Monte Carlo Generator, Nucl. Instrum. Meth. A614, 87 (2010).

[12] C. Hagmann, D. Lange, and D. Wright, Cosmic-ray shower generator (CRY) for Monte Carlo transport codes, in Nuclear Science Symp. Conf. Rec. (Honolulu, HI) volume 2, pages 1143–1146 IEEE 2007.

[13] S. Agostinelli et al., Geant4 - A Simulation Toolkit, Nucl. Instrum. Meth. A506, 250 (2003).

[14] J. Allison et al., Geant4 Developments and Applications, IEEE Trans. Nucl. Sci. 53, 270 (2006).

[15] [*) L.Kolupaeva, K.Kuzmin, O.Petrova, I.Shandrov, Mod.Phys.Lett. A31 (2016) no.12, 1650077

[16] [*) K.Kuzmin, V.Naumov, O.Petrova, Acta Phys.Polon.Supp. 9 (2016) 795-796

[17] J. N. Capdevielle, C. Le Gall, K. N. Sanosian,"Simulation of extensive air showers at ultrahigh energy using the CORSIKA Monte Carlo code", Astropart. Phys. 13, 259 (2000).

[18] R. P. Kokoulin, A. A. Petrukhin, Phys. Part. Nucl. (Zh. Fiz. Elem. Chast. Atom. Yadra) (In russian), 21, no. 3, 774 (1990).

[19] C. Patrignani et al. (Particle Data Group), Chin. Phys. C, 40, 100001 (2016).

[*) marks physics publications with JINR NOvA project authors

8. Conference Presentations and Seminars given by JINR team members

1) L.Kolupaeva, *Measurements for neutrino mass hierarchy and delta CP from the NOvA experiment*, DLNP neutrino seminar, 17 March 2017.
2) O.Samoylov, *Measurement for theta23 in the NOvA experiment*, DLNP neutrino seminar, 03 March 2017.
3) O.Samoylov, *SA results from the NOvA experiment*, DLNP neutrino seminar, 21 December 2016.
4) A.Sheshukov *Supernova neutrino detection in NOvA experiment*, Poster on Neutrino-2016, London, 4-9 July 2016.
5) I.Kakorin et al., *Running axial mass for quasielastic neutrino-nucleus scattering*, NuTune2016, Liverpool, Great Britain, July, 2016.
6) L.Kolupaeva, *Current results of the NOvA experiment*, plenary talk on 19th International Seminar on High Energy Physics QUARKS-2016, 29 May – 04 June 2016.
7) O.Samoylov et al., *Remote operation center at Dubna for the NOvA experiment*, AYSS-2016, Dubna 14-18 March 2016 and GRID-2016, Dubna, 5 July 2016.
8) N.Balashov et al., *JINR LIT resources for NOvA experiment*, AYSS-2016, Dubna 14-18 March 2016 and Poster on The 2016 European School of High-Energy Physics, Skeikampen, Norway, 15-28 June 2016.
9) A.Antoshkin et al., *NOvA test bench at JINR*, AYSS-2016, Dubna 14-18 March 2016.
10) L.Kolupaeva, *Matter effect in neutrino oscillations for NOvA experiment*, AYSS-2016, Dubna 14-18 March 2016 and young scientist talk on 120th JINR Scientific Council, 23 September 2016.
11) L.Kolupaeva, *NOvA sensitivities after first year of running*, Lomonosov-2016, 11-15 April 2016.
12) O.Samoylov, Current results of the NOvA experiment, ICSSNP, Neutrino Physics, Dubna, 12-15 April 2016.
13) O.Petrova et al., *Quasielastic neutrino-nuclei interactions and the approach of running nucleon axial mass*, ICSSNP, Neutrino Physics, Dubna, 12-15 April 2016.
14) O.Samoylov, First results from the NOvA experiment, DLNP neutrino seminar, 18 September 2015.
15) L.Kolupaeva et al., *Some uncertainties of neutrino oscillation effect in the NOvA experiment*, 6th summer Pontecorvo school on neutrino physics, 27 August - 04 September 2015.
16) O.Petrova et al., *Neutrino-nuclear interactions for neutrino oscillation in NOvA*, Alushta-2105, June 2015.
17) O.Samoylov, Neutrino oscillation in accelerator experiments (NOvA/T2K) and in reactor experiments (JUNO), ISU seminar, Irkutks, September 2014.
18) O.Petrova et al., *The effective nucleon axial mass approach and quasielastic neutrino event rates in NOvA and Super-Kamiokande*, Flavour Physics Conference (Xth Rencontres du Vietnam), International Center of Interdisciplinary Science Education (ICISE), Quy Nhon, Vietnam, 2014
19) O.Petrova et al., *The effective nucleon axial mass approach and quasielastic neutrino event rates in the Near Detector of NOvA*, 18th International Seminar on High Energy Physics (QUARKS-2014), INR RAS Moscow, JINR Dubna, Suzdal, Russia, 2014.
20) O.Petrova et al., *The effective nucleon axial mass approach and quasielastic neutrino event rates in the Super-Kamiokande*, AYSS-2014, February 2014 and ESHEP2014.
21) O.Samoylov, *Status of the NOvA experiment*, Prospects of Particle Physics: Neutrino Physics and Astrophysics, Valdai, January 2014.
22) O.Petrova et al. *Impact of the nucleon axial mass uncertainty on evaluation of the quasielastic neutrino event rate in the Super-Kamiokande detector*, 16th International Moscow School of Physics (41th ITEP Winter School of Physics), 2013.
23) O.Samoylov, *Neutrino oscillation in the NOvA experiment*, DLNP neutrino seminar, November 2013.

Предлагаемый план-график и необходимые ресурсы для осуществления проекта NOvA

Наименование узлов и систем установки, ресурсов, источников финансирования			Стоимость узлов установки (тыс.долл.) Потребности в ресурсах	Предложения Лабор распределению фина и ресурсов		
				1 год	2 год	3 год
Основные узлы и оборудова ние	1. Модернизация Virtual Control Room в ОИЯИ, связь, замена части компьютеров и офисного оборудования, расходные материалы		30.0	10.0	10.0	10.0
	2. Лабораторное оборудование для измерений и тестов электроники и сцинтиллятора (крейт, генератор, блоки электроники и другие)		15.0	5.0	5.0	5.0
	3. Вычислительная инфраструктура (вычислительные серверы, диски для хранения данных)		195.0	65.0	65.0	65.0
Необходи мые ресурсы	*нормо-часы*	ОП ОИЯИ ООЭП ЛЯП	*2100 2400*	*700 800*	*700 800*	*700 800*
	тыс. долл.	Визиты в Fermilab, конферен ции и другие совещани я	180.0	60.0	60.0	60.0
Источники финансир ования	Бюджет	Затраты из бюджета	**390.0**	**130.0**	**130.0**	**130.0**
	Внебюджетны е средства	Вклады коллаборан тов, средства по грантам и другие	**30.0**	**10.0**	**10.0**	**10.0**

Руководитель проекта

Смета затрат по проекту NOvA

№№ пп	Наименование статей затрат	Полная Стоимость Нормочасы Тыс. долл.	1 год	2 год	3 год
1.	Ускоритель	-	-	-	-
2.	ЭВМ	-	-	-	-
3.	Комп. связь (тыс. долл.)	6.0	2.0	2.0	2.0
4.	*ООЭП ЛЯП (нормочасы)*	*2400*	*800*	*800*	*800*
5.	*ОП ОИЯИ (нормочасы)*	*2100*	*700*	*700*	*700*
6.	Материалы (тыс. долл.)	9.0	3.0	3.0	3.0
7.	Оборудование (тыс. долл.)	225.0	75.0	75.0	75.0
8.	Оплата НИР (тыс. долл.)	-	-	-	-
9.	Командировочные расходы (тыс. долл.)	150.0	50.0	50.0	50.0
	Итого по прямым расходам (тыс. долл.)	**390.0**	**130.0**	**130.0**	**130.0**

Руководитель Проекта

Директор Лаборатории

**Ведущий инженер-экономист
Лаборатории**